Nature and significance of Late Cretaceous ophiolitic rocks and their relation to the Baskil granitic intrusions of the Elazığ region, SE Turkey

TAMER RIZAOĞLU[1], OSMAN PARLAK[1], VOLKER HOECK[2] & FİKRET İŞLER[1]

[1]*Çukurova Üniversitesi, Jeoloji Mühendisliği Bölümü, 01330 Balcalı, Adana, Turkey (e-mail: parlak@cukurova.edu.tr)*

[2]*University of Salzburg, Department of Geology, A-5020 Salzburg, Austria*

Abstract: The Elazığ region in SE Turkey comprises, in descending order, the Palaeozoic–Mesozoic Malatya–Keban platform, an ensimatic island arc unit (i.e. Elazığ magmatic rocks–Yüksekova complex), and ophiolitic rocks (i.e. Kömürhan) of Late Cretaceous age. All of these were intruded by the Baskil granitic rocks. These tectonomagmatic–stratigraphic assemblages were emplaced over the Middle Eocene volcano-sedimentary Maden complex to the south during the evolution of the SE Anatolian orogen. The Kömürhan ophiolite exhibits an intact ophiolite pseudostratigraphy. The base of this has been metamorphosed to amphibolite facies during intraoceanic subduction–thrusting. The amphibolitic rocks were intruded by synkinematic granitic rocks (Baskil magmatic rocks). The ensimatic island arc volcanic rocks are widely distributed in the region. The contact of the volcano-sedimentary unit with the underlying Kömürhan ophiolite is a thrust dipping to the north. The rock assemblages of the volcano-sedimentary unit suggest formation of small volcanic edifices above a subduction zone, coupled with debris-flow deposits and volcaniclastic turbidites. The whole-rock and mineral chemistry of the Kömürhan ophiolite and the ensimatic island arc volcanic rocks suggests that they represent a comagmatic tholeiitic suite, formed in the Late Cretaceous in a suprasubduction zone (SSZ) setting. The amphibolites beneath the Kömürhan ophiolite indicate derivation from an island arc tholeiite (IAT) protolith. The geological and geochemical evidence from the Elazığ region suggests the following evolutionary scenario. The Kömürhan ophiolite was formed above a north-dipping subduction zone between the Arabian platform to the south and the Tauride platform to the north in Late Cretaceous (*c*. 90 Ma). An ensimatic island arc assemblage was then built on the SSZ-type crust. The metamorphic sole was formed by metamorphism of IAT-type basalts that were detached from the front of the overriding Kömürhan ophiolite and then underplated. These units were then accreted to the base of the Tauride active margin to the north, where both units were cut by the Baskil granitic rocks around 85 Ma.

Anatolia is situated in a critical segment of the Alpine–Himalayan orogenic system, where remnants of Neotethyan ocean basins crop out along east–west-trending tectonic zones located between metamorphic massifs or platform carbonates (Şengör & Yılmaz 1981; Yılmaz *et al.* 1993; Robertson 2002). The remnants of Neotethys are characterized, in a structural descending order, by ophiolites, metamorphic soles and ophiolitic mélanges (Fig. 1). The ophiolites and related subduction–accretion units were generated during the closing stages of Neotethyan oceanic basins in the Late Cretaceous (Pearce *et al.* 1984; Yalınız *et al.* 1996, 2000; Robertson 2002, 2004; Parlak & Robertson 2004; Parlak *et al.* 2004; Robertson *et al*. 2006, 2007). The Late Cretaceous ophiolites in Turkey are located in five zones based mainly on their geographical distribution; namely, the Pontide ophiolite belt, the Central Anatolian ophiolite belt, the Tauride ophiolite belt, the SE Anatolian ophiolite belt and the Peri-Arabian ophiolite belt (Fig. 1).

The SE Anatolian orogenic belt is one of the best regions to study mountain-building processes resulting from the collision of the Afro-Arabian and Eurasian plates in Mid-Miocene time (Yılmaz 1993; Yılmaz *et al.* 1993). The ophiolites, ensimatic island arc units, ophiolite-related metamorphic rocks and granitic rocks within this orogenic belt are important elements of the Late Cretaceous tectonomagmatic evolution of the southern Neotethys. The Late Cretaceous ophiolites are the Göksun (Kahramanmaraş or N Berit), İspendere (Malatya), Kömürhan and Guleman ophiolites (Elazığ). The ensimatic island arc volcanic unit is represented by either the Elazığ magmatic rocks or the Yüksekova complex. The ophiolite-related metamorphic units are the Berit metaophiolite (S Berit ophiolite) and the metamorphic sole of the

From: ROBERTSON, A. H. F. & MOUNTRAKIS, D. (eds) 2006. *Tectonic Development of the Eastern Mediterranean Region*. Geological Society, London, Special Publications, **260**, 327–350.
0305-8719/06/$15.00

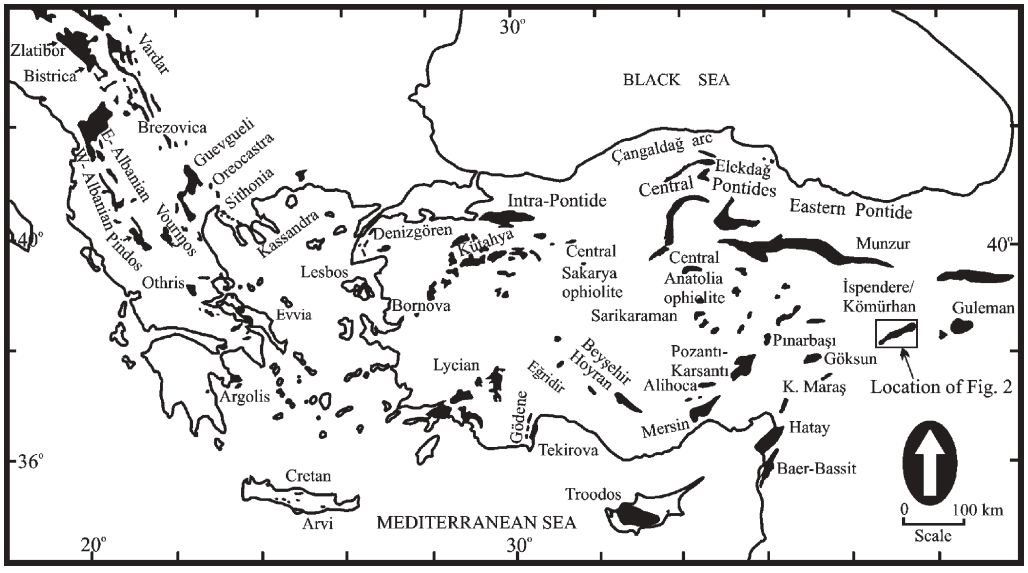

Fig. 1. Distribution of the Neotethyan ophiolites in the eastern Mediterranean region (from Robertson 2002).

Kömürhan ophiolite. The granitic rocks are located in three different areas: the Göksun–Afşin (Kahramanmaraş), Doğanşehir (Malatya) and Baskil (Elazığ) regions. The petrology and geochronology of the Göksun (N Berit) ophiolite and related granitic rocks to the north of Kahramanmaraş are well constrained (Parlak *et al.* 2004; Parlak 2006; Robertson *et al.* 2006, 2007). However, the relations of the Late Cretaceous tectonomagmatic units in the Elazığ region are not well established because of very limited geochemical and geochronological data. The main uncertainty in the Late Cretaceous evolution of the region is the relationships between the Baskil granitic body, the Elazığ magmatic rocks–Yüksekova complex and the Kömürhan ophiolite. One interpretation is that the Elazığ magmatic rock units are the extrusive equivalents of the Baskil arc plutonic rocks that represent an Andean-type active margin along the Malatya–Keban platform to the north; the Kömürhan ophiolite formed away from the Tauride margin to the south (i.e more oceanic) in this model (Yazgan & Chessex 1991). A second interpretation is that the Elazığ magmatic unit, comprising both intrusive and extrusive rocks, is an island arc assemblage. This island arc unit formed above the Kömürhan ophiolite during a mature stage of suprasubduction zone (SSZ) spreading (Beyarslan & Bingöl 1996, 2000). A third interpretation is that the extrusive rocks in the Elazığ region have nothing to do with the Baskil arc plutonic rocks and could be seen as the westward continuation of the Yüksekova ensimatic island arc unit formed above a subduction zone during the Late Cretaceous (Perinçek 1979; Aktaş & Robertson 1984).

More recently, geological mapping was carried out in the area between Baskil and Sivrice (Elazığ) regions (see Fig. 3) to investigate the field relations of the tectonomagmatic units. A detailed stratigraphic log was measured of the ensimatic island arc volcanic unit (Elazığ magmatic rocks–Yüksekova complex). This paper presents whole-rock and mineral chemical data for the Kömürhan ophiolite and the ensimatic island arc unit from the Elazığ region; the results can be interpreted in terms of the spatial and temporal relations between the tectonomagmatic units and the Baskil granitic body during the Late Cretaceous.

Regional geology

The Malatya–Elazığ region comprises a number of tectonomagmatic–stratigraphic units that are important for the evolution of the southern Neotethyan ocean. These are the Malatya–Keban metamorphic unit, the Pütürge metamorphic unit, Late Cretaceous ophiolites, the Baskil arc magmatic unit, the Elazığ magmatic unit, the Maden unit and sedimentary cover units (Fig. 2). The Malatya–Keban metamorphic unit is a low-grade metamorphosed Late Palaeozoic–Mesozoic unit consisting of marble, schist, slate and black phyllite, with rare metaconglomerates (Asutay 1988; Turan & Bingöl 1991; Yılmaz *et al.*

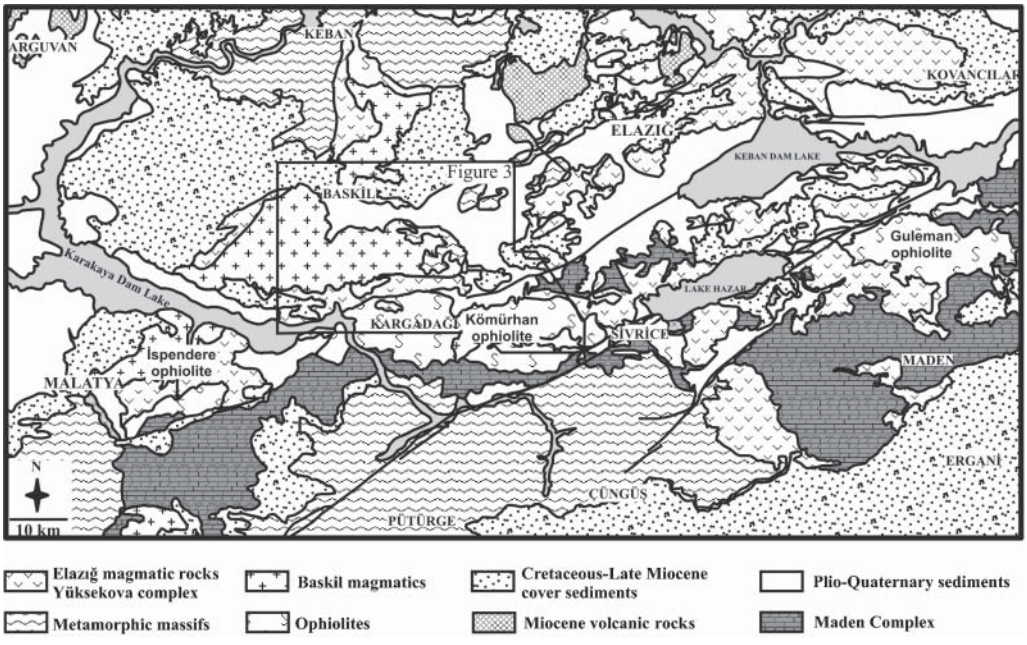

Fig. 2. Regional geological map of the Elazığ region (MTA 2002).

1993). It has both tectonic and intrusive contact relationships with the Baskil arc magmatic unit and is, in turn, overlain by Tertiary unmetamorphosed sedimentary rocks in the Elazığ region (Bingöl 1984; Yazgan & Chessex 1991; Rızaoğlu *et al.* 2004). The Pütürge metamorphic unit comprises both core and cover units. The core rocks are dominated by augen gneiss, amphibole schist and biotite schist with an intruding granite (Yılmaz 1971, 1978), whereas the cover rocks consist of slates, phyllites, calc-schists and marbles (Yılmaz *et al.* 1993; Erdem & Bingöl 1995). The Pütürge metamorphic unit is unconformably overlain by the Middle Eocene Maden unit. Yılmaz *et al.* (1993) believed that, the metamorphism of the Malatya–Keban and Pütürge units occurred during the Campanian to Early Maastrichtian interval because the uppermost units of the metamorphic sequences are Campanian in age (Yılmaz *et al.* 1987) and the massifs are unconformably overlain by an Upper Maastrichtian sedimentary cover.

The Baskil arc magmatic unit is mainly exposed near Baskil town and to the north of Keban Lake (Fig. 2) where it cuts the Malatya–Keban platform, the Elazığ magmatic unit–Yüksekova complex and the Kömürhan ophiolite (Parlak 2006). This magmatic complex was interpreted as I-type calc–alkaline intrusive rocks formed as a result of ensimatic island arc–continent collision during closure of the southern Neotethys. It is represented by basic to silicic plutonic rocks and swarms of dykes. K–Ar ages from the Baskil intrusive rocks are reported as 76 ± 2.45 and 78 ± 2.5 Ma by Yazgan & Chessex (1991).

The Maden group is a low-grade metamorphosed volcanic and sedimentary unit of Mid-Eocene (Ypresian–Lutetian) age that crops out to the south of Elazığ region (Fig. 2). It unconformably overlies the Pütürge metamorphic unit and is, in turn, tectonically overlain by ophiolites (Fig. 2). There is no consensus on the nature of the Maden Group. Various interpretations were proposed, such as an immature island arc association (Erdoğan 1977), a product of intracontinental subduction (Yazgan 1983, 1984; Michard *et al.* 1985), a back-arc basin (Şengör & Yılmaz 1981; Hempton 1984, 1985), or an immature back-arc basin (Yiğitbaş & Yılmaz 1996*a, b*).

The Elazığ magmatic unit is a basic to silicic volcanic and volcano-sedimentary rock assemblages of Late Cretaceous age. It is widely distributed around the Keban Lake and Elazığ town

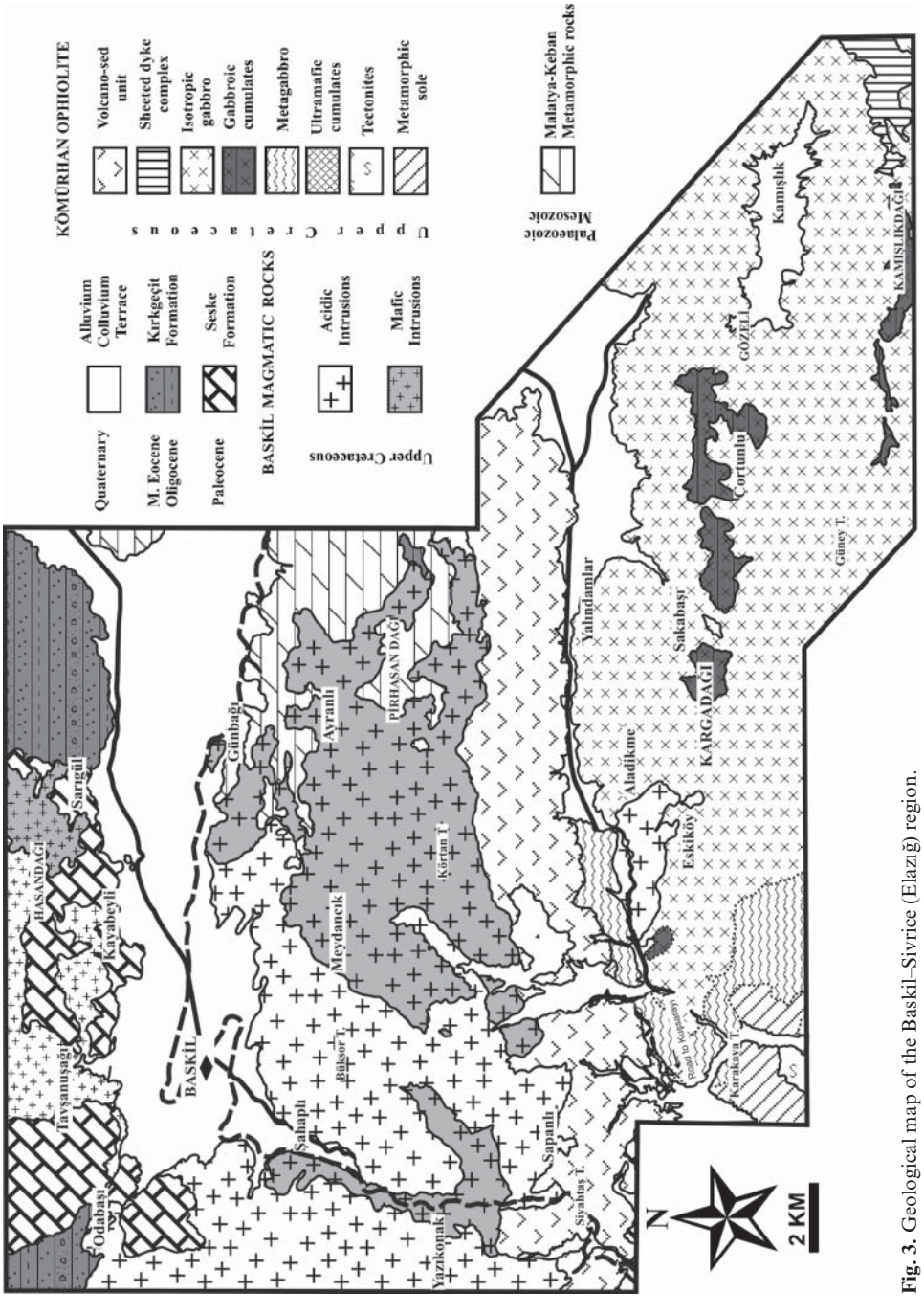

Fig. 3. Geological map of the Baskil–Sivrice (Elazığ) region.

(Fig. 2). This unit has been interpreted as the extrusive equivalents of the Baskil arc plutonic rocks (Yazgan & Chessex 1991; Beyarslan & Bingöl 1996, 2000), or an ensimatic volcanic arc unit–Yüksekova complex (Perinçek 1979; Aktaş & Robertson 1984). Recently, based on field and geochemical data, Rızaoğlu *et al.* (2004) showed that this volcanic and sedimentary rock assemblage has a thickness of *c*. 750 m and has a tholeiitic nature. They interpreted this unit as the extrusive part of the Kömürhan ophiolite which was formed in an SSZ environment in the Late Cretaceous.

The ophiolites in the region, from west to east, are represented by the İspendere, Kömürhan and Guleman ophiolites (Fig. 2). The Kömürhan is distinct as the lower part of the ophiolite pseudostratigraphy is metamorphosed (Yazgan & Chessex 1991). These ophiolites are interpreted as the emplaced remnants of southern Neotethys formed above a subduction zone (Perinçek 1979; Aktaş & Robertson 1984; Beyarslan 1996; Beyarslan & Bingöl 2000).

Field relations and petrography

The Baskil granitic rocks are represented by mafic to acidic plutonic rocks (diorite, granodiorite, granite, tonalite, quartz diorite, quartz monzonite) and swarms of dykes (aplite, diabase, microdiorite and granophyre). It has both tectonic and intrusive contact relationships with the Malatya–Keban platform in the central part of the study area near Ayranlı (Fig. 3). The Baskil intrusive rocks are unconformably overlain by Palaeocene and younger sediments between Odabaşı and Hasandağı (Fig. 3), whereas they intrude the Kömürhan unit and the volcano-sedimentary unit to the south (Fig. 3). The Kömürhan ophiolite comprises a complete oceanic lithospheric remnant and is represented, from the bottom to the top, by mantle tectonites, ultramafic–mafic cumulates, isotropic gabbros, sheeted dykes, volcanic rocks and associated sedimentary rocks (Fig. 4). A thin metamorphic sole unit tectonically underlies the mantle tectonites to the south of Karakaya Tepe (Fig. 3).

The volcano-sedimentary unit of the Kömürhan ophiolite crops out along an east–west-trending belt in the central part of the study area (Fig. 3). It is represented by alternations of volcanic and sedimentary rock units and has a thickness of *c*. 750 m (see Fig. 5). At the base, the volcanic section has a sharp tectonic contact with the plutonic rocks (gabbro) of the Kömürhan ophiolite, as seen along the Baskil–Kuşsarayı road, and is intruded by the Baskil granitic rocks at Sapanlı and south of Kargadağı (Fig. 3). Massive to stratified lithologies of the volcanic section are pillow lavas, lava breccias, massive lava flows, debris flow, alternations of volcanogenic sandstone and siltstone, siliceous tuff, mudstone–limestone alternations and columnar-jointed lava flows (Fig. 5). The volcanic rocks are characterized by basalt, basaltic andesite, andesite, dacite and rhyodacite including secondary gypsum as veins and massive sulphfide deposits (Bölücek *et al*. 2004) (see Fig. 5). The basalts display amygdaloidal, intersertal, hyalomicrolitic porphyritic to microlitic porphyritic textures and are dominated by plagioclase and pyroxene-phyric lavas. The andesites show amygdaloidal, hyalomicrolitic porphyritic to microlitic porphyritic textures and are plagioclase and amphibole-phyric lavas. The rhyodacites display microlitic porphyritic to microgranular porphyritic textures, and are represented by plagioclase-phyric lavas. Plagioclase is seen either as phenocrysts or as microliths within the matrix. Euhedral to subhedral corroded quartz forms phenocrysts. Dacites show hyalo-porphyritic to amygdaloidal textures and are dominated by zoned plagioclase and corroded quartz set in a fine-grained matrix. Common secondary phases in the volcanic rocks are epidote, chlorite, calcite, albite, kaolinite and opaque minerals.

The sheeted dyke complex of the Kömürhan ophiolite is represented by diabase, microdiorite and quartz microdiorite, and is well preserved in the eastern part of the study area, east of Kamışlıkdağ (Figs 3 and 4). Individual dykes exhibit variable thicknesses ranging from 15–20 cm to 100–150 cm, without obvious chilled margins. The dykes display intergranular, doleritic and microgranular textures. The main mineral phases are plagioclase, pyroxene, amphibole, quartz and magnetite. The sheeted dyke rocks are often associated with secondary calcite, amphibole, chlorite and epidote.

The isotropic gabbros of the Kömürhan ophiolite crop out extensively in the southern part of the study area, between Eskiköy and Kamışlık (Figs 3 and 4), and are represented by gabbro, diorite and quartz diorite. Gabbros display a non-cumulus granular to poikilitic texture and are characterized by primary plagioclase ($An_{55–60}$) (60–70 vol.%), clinopyroxene (15–20 vol.%), orthopyroxene (<5 vol.%) and opaque minerals (Fe–Ti oxide). Diorites exhibit granular to intergranular texture and are represented by plagioclase ($An_{35–40}$) (60–70 vol.%), amphibole (30 vol.%), quartz (*c*. 1 vol.%) and opaque minerals (Fe–Ti oxide). Quartz diorites display granular textures and comprise slightly zoned plagioclase (50 vol.%), amphibole (25 vol.%), quartz (15–20 vol.%) and opaque minerals (Fe–Ti oxide). The

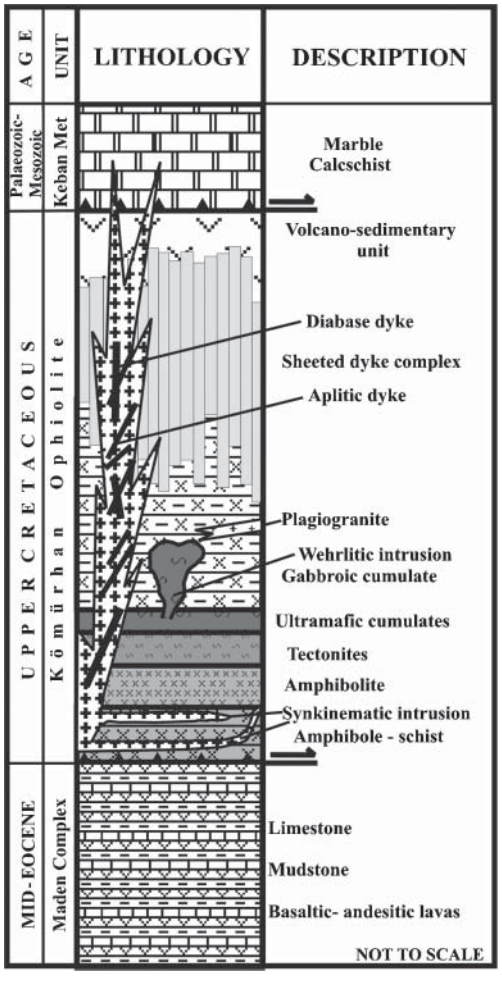

Fig. 4. Tectonomagmatic–stratigraphic units in Baskil–Sivrice (Elazığ) region.

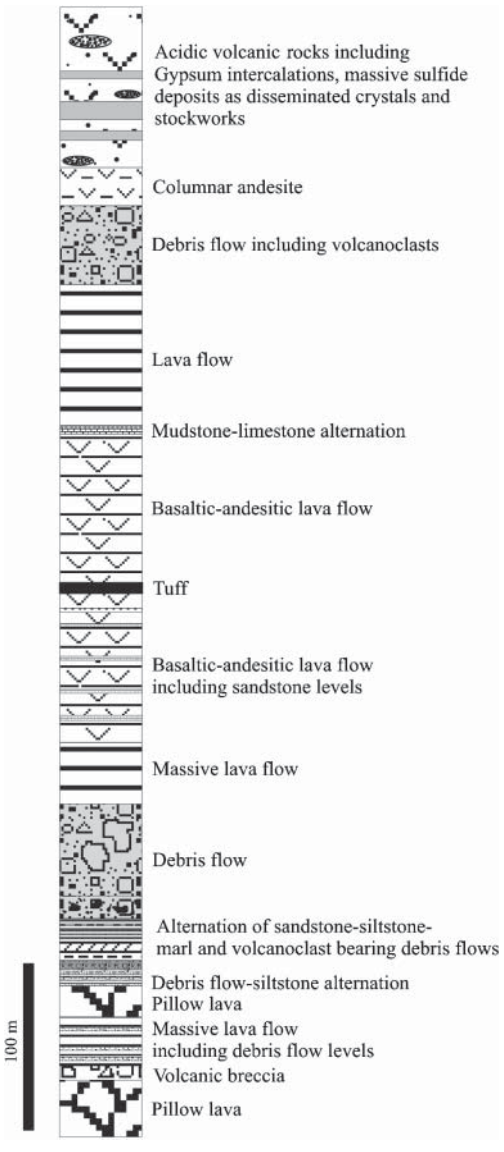

Fig. 5. Measured stratigraphic section from the volcano-sedimentary rocks of the Kömürhan ophiolite.

rock isotropic gabbros include secondary calcite, chlorite, epidote and kaolinite.

The ultramafic to mafic cumulate rocks of the Kömürhan ophiolite crop out at Karadağı, Çortunlu and Kamışlıkdağ (Fig. 3). Ultramafic cumulates consist of wehrlite, whereas mafic cumulates are represented by olivine gabbro, gabbro–norite, gabbro and amphibole gabbro. The wehrlite displays a granular texture and is represented by olivine (60–70 vol.%), clinopyroxene (20–30 vol.%) and chromite (1–2 vol.%). The olivines and pyroxenes in the wehrlites are serpentinized to variable degrees. The olivine gabbro displays granular to poikilitic textures: it comprises olivine ($Fo_{73–76}$; 20–30 vol.%) with a grain size of 1–6 mm, plagioclase ($An_{92–94}$; 50–80 vol.%) with a grain size of 0.4–7 mm, clinopyroxene ($En_{69–70}Wo_{22–27}Fs_{4–8}$; 5–30 vol.%) with a grain size of 1–4 mm, orthopyroxene ($En_{76–77}Wo_{0.6–0.7}Fs_{22–23}$; <5 vol.%) with a grain size of 1–5 mm, chromite and Fe–Ti oxide minerals. Serpentine, chlorite, talc, epidote and amphibole are secondary phases. The gabbronorite displays granular to poikilitic textures and is characterized by clinopyroxene ($En_{40–51}Wo_{21–44}Fs_{7–26}$; 20–30 vol.%) with a grain size of 0.5–3 mm, orthopyroxene ($En_{57–61}Wo_{1.3–2.2}Fs_{37–40}$;

10–15 vol.%) with a grain size of 0.5–2.5 mm, plagioclase ($An_{53–77}$; *c*. 50 vol.%) with a grain size of 0.5–4 mm and opaque (Fe–Ti oxide) minerals. The gabbro displays granular to poikilitic textures and is characterized by plagioclase (60–80 vol.%) with a grain size of 0.5–7.5 mm, clinopyroxene (15–20%) with a grain size of 1–7 mm, orthopyroxene (1–2%) and amphibole (3–5%). Kaolinite, sericite, chlorite and magnetite are secondary phases. The amphibole gabbro has a granular to poikilitic texture and is represented by plagioclase ($An_{43–57}$; 80–85%), amphibole (10–15%), biotite (2–3%) and opaque minerals (1–2%).

Mantle tectonites within the Kömürhan ophiolite are very limited, and are observed only in the SW of the study area (Fig. 3). The rock units are of serpentinized dunite, harzburgite, lherzolite and serpentinite.

The metamorphic sole rocks crop out in the southwestern end of the study area especially south of Karakaya Tepe (Figs 3 and 4) where they have a tectonic contact with the mantle tectonites. They are cut by synkinematic granites near Kömürhan bridge. The metamorphic sole is represented by amphibolite, plagioclase amphibolite, plagioclase–epidote–amphibole schist, quartz–plagioclase–amphibole schist and metasediments. The amphibolites exhibit granoblastic texture and comprise coarse-grained magnesio-hornblendes. The plagioclase amphibolites show granoblastic to grano-nematoblastic texture and are represented by plagioclase (20–25%), amphibole (70–75%) and accessory sphene and magnetite minerals. The plagioclase–epidote–amphibole schists display banded to nematoblastic textures and comprise amphibole (50–60%), epidote (15–20%), plagioclase (5–10%), secondary chlorite and magnetite. The quartz–plagioclase–amphibole schists exhibit banded to nematoblastic textures, and are characterized by amphibole (70–75%), plagioclase (*c*. 20%), quartz (*c*. 5%) and accessory sphene and magnetite.

Geochemistry

Analytical methods

A total of 75 samples from the metamorphic sole (11), cumulate (19), isotropic gabbro (six), sheeted dyke (15) and volcanic rocks (24) of the Kömürhan ophiolite were analysed for major and trace elements by standard X-ray fluoresence (XRF) spectrometry. Major element contents were determined on glass beads fused from ignited powders to which $Li_2B_4O_7$ was added at a ratio of 1:5, in a gold–platinum crucible at 1150 °C. Trace element contents were measured by XRF on pressed-powder pellets. A subset of 29 samples were also analysed for trace elements (including rare earth elements (REE)) by inductively coupled plasma–mass spectrometry (ICP-MS) at Acme Analytical Laboratories in Canada. The results of the analyses are presented in Tables 1 and 2. A total of eight representative polished sections were used for electron microprobe analysis on a JEOL JXA-8600 instrument in the Geology and Paleontology Department at Salzburg University (Austria). The analytical conditions for the elements were a counting interval of 13 s (10 s for peak and 3 s for background), a beam current of 20 nA and an acceleration voltage of 15 kV. The data reduction was done following the ZAF procedure. Fe^{3+} and Fe^{2+} were determined from stoichiometry of spinel using the equation of Droop (1987). The results of the analyses are presented in Tables 3–5.

Whole rock

Major, trace and rare earth elements are given in Tables 1 and 2 for the volcanic, sheeted dyke, isotropic gabbro, cumulate and metamorphic sole rocks of the Kömürhan ophiolite. Loss on ignition (LOI) values reach 9.12% in the volcanic rocks, 2.41% in the sheeted dykes, 3.21% in the isotropic gabbros and 4.1% in the metamorphic sole rocks, reflecting variable secondary alteration, which is indicated by the presence of mineral phases such as epidote, calcite or chlorite. The mobility of many elements during low-grade submarine alteration has been well constrained by a number of studies (e.g. Hart *et al.* 1974; Humphries & Thompson 1978). For this reason, recourse is generally made to relatively immobile elements such as Ti, P, Zr, Y, Nb and REE, and to a lesser extent Cr, Ni, Sc and V, to designate lava groups, petrogenetic trends and tectonic environments (Pearce & Cann 1973; Floyd & Winchester 1975, 1978; Pearce & Norry 1979). The rock classification diagram for the rock units of the Kömürhan ophiolite is based on Zr/Ti v. Nb/Y (Pearce 1996). The lavas cover a wide compositional range from basalt to rhyodacite, but basaltic to andesitic compositions predominate (Fig. 6a). The sheeted dykes are characterized by diabase and microdiorite, whereas the isotropic gabbros are dominated by gabbroic rocks (Fig. 6b and c). The amphibolites of the metamorphic sole reflect their derivation from a basaltic protolith (Fig. 6d). Nb/Y ratios are in the range of 0.5–0.02 in volcanic rocks, 0.19–0.09 in sheeted dykes, 0.2–0.06 in isotropic gabbros and 0.33–0.07 in metamorphic sole rocks, indicating that all the analysed rocks from the Kömürhan ophiolite are tholeiitic in character (Pearce 1982)

Table 1. *Major and trace element contents of rock samples from the Kömürhan ophiolite*

	Volcanic rocks							Sheeted dykes				Isotropic gabbro			Cumulate rocks					Metamorphic sole		
Sample:	B-471	B-480	B-490	B-492	B-627	B-474	B-615	B-499	B-513	B-504	B-506	B-503	B-572	B-583	B-341	B-406	B-603	B-315	B-314	B-338	B-347	B-354
SiO_2	47.54	57.43	55.93	60.48	53.28	77.87	62.47	58.63	54.74	51.76	48.78	49.66	60.83	50.34	49.07	40.57	47.50	44.42	40.35	47.16	45.94	49.26
TiO_2	1.43	0.73	0.72	1.12	0.98	0.21	0.49	1.65	1.68	1.91	1.20	0.54	0.24	0.20	1.12	0.21	0.26	0.15	0.08	1.02	1.00	0.47
Al_2O_3	15.46	16.48	16.88	15.09	17.73	12.02	15.79	14.36	15.17	14.79	14.54	17.05	14.81	18.39	18.26	24.56	16.58	17.73	5.73	18.85	15.63	8.69
FeO*	11.20	7.00	7.79	10.60	8.33	2.45	4.87	8.29	7.32	13.55	10.62	7.50	4.91	5.54	11.75	9.81	6.28	4.27	10.34	11.12	10.39	9.00
MnO	0.31	0.10	0.15	0.17	0.18	0.05	0.08	0.04	0.03	0.21	0.20	0.14	0.12	0.11	0.24	0.12	0.11	0.09	0.14	0.20	0.18	0.18
MgO	4.47	4.49	4.62	1.68	2.96	0.04	0.80	2.84	3.53	5.60	7.49	7.61	5.54	8.56	4.53	10.04	11.72	11.28	30.35	5.88	9.34	15.88
CaO	8.17	2.95	5.39	5.09	5.03	0.65	4.23	7.45	8.80	4.52	9.82	13.17	8.72	13.27	9.44	13.17	14.42	18.19	6.09	10.83	12.09	13.22
Na_2O	5.43	6.20	2.43	4.14	0.68	6.26	2.57	5.35	6.21	5.54	3.42	2.38	2.42	2.11	3.22	0.36	1.12	0.58	0.07	2.43	1.74	0.62
K_2O	0.33	0.79	1.57	0.47	2.60	0.08	2.74	0.11	0.06	0.10	0.22	0.04	0.86	0.11	0.38	0.01	0.10	0.15	0.01	1.02	0.41	0.38
P_2O_5	0.16	0.17	0.16	0.17	0.12	0.04	0.12	0.38	0.38	0.17	0.09	0.03	0.02	0.01	0.26	0.01	0.02	0.01	0.02	0.18	0.08	0.06
LOI	5.49	3.69	4.30	1.22	7.47	0.67	5.49	1.12	0.86	2.15	2.28	2.13	1.22	0.82	0.68	0.83	1.84	2.88	6.97	1.43	3.58	2.03
Cr_2O_3	0.01	0.01	0.00	0.00	0.00	0.00	0.00	0.00	0.01	0.00	0.03	0.02	0.02	0.08	0.00	0.03	0.11	0.20	0.16	0.00	0.04	0.24
NiO	0.00	0.00	0.00	0.00	0.00	0.00	0.00	0.00	0.00	0.00	0.01	0.01	0.01	0.02	0.00	0.01	0.03	0.04	0.13	0.00	0.01	0.04
Total	100.00	100.04	99.94	100.23	99.36	100.33	99.65	100.20	98.77	100.28	98.69	100.28	99.71	99.56	98.95	99.72	100.08	99.99	100.43	100.11	100.44	100.07
Nb	4	4	4	4	1	5	15	7	6	6	4	1	2	1	3	1	1	1	7	3	2	6
Zr	95	62	79	59	83	126	200	253	293	102	67	24	24	10	71	10	16	9	16	46	37	25
Y	33	24	24	21	27	49	38	69	70	36	27	16	10	8	30	4	12	8	6	28	25	18
Sr	332	485	355	232	49	49	75	124	132	78	295	128	154	169	388	375	107	513	19	290	182	102
U	2	2	2	2	2	2	4	2	2	2	2	2	2	2	2	2	2	2	2	2	2	2
Rb	7	8	18	5	82	2	103	2	3	3	4	3	21	5	3	3	7	7	4	29	10	8
Th	2	4	5	2	2	3	7	2	3	2	2	2	6	2	2	2	2	2	2	2	2	3
Pb	3	5	9	8	3	7	4	2	2	7	10	15	15	15	12	16	18	19	33	17	15	26
Ga	20	16	18	14	19	12	19	18	20	21	18	16	12	12	21	15	11	10	6	20	16	10
Ni	27	19	5	5	9	2	2	11	17	12	45	49	39	111	3	74	167	251	633	21	83	237
Co	40	24	23	31	27	2	6	19	16	42	46	39	23	35	30	60	44	37	106	37	47	51
Cr	77	69	8	2	3	2	2	19	57	3	258	154	139	541	4	153	740	1483	1081	20	307	1833
V	411	237	227	416	390	16	26	139	232	426	274	201	127	110	350	151	130	95	64	330	286	223
Ce	18	53	34	10	18	35	41	36	37	27	10	5	10	11	26	9	20	12	26	20	15	20
Nd	7	15	14	4	7	9	21	14	14	7	4	4	4	6	17	4	13	9	5	13	8	9
Ba	30	228	222	66	110	69	351	40	42	32	30	11	276	69	135	9	14	148	21	325	120	55
La	4	11	15	6	4	5	29	4	6	4	4	4	10	4	11	4	4	4	4	7	10	22
Hf	4	4	4	4	4	5	6	6	9	6	3	4	2	1	1	3	1	1	1	2	1	1
Sc	32	33	33	26	40	5	9	20	15	58	44	28	26	19	36	21	26	13	64	29	36	55
Nb/Y	0.12	0.17	0.17	0.19	0.04	0.10	0.39	0.10	0.09	0.17	0.15	0.06	0.20	0.13	0.10	0.25	0.08	0.13	1.17	0.11	0.08	0.33
Mg-no.	28.53	39.06	37.24	13.68	26.21	1.59	14.17	25.51	32.54	29.23	41.37	50.39	53.02	60.69	27.82	50.57	65.10	72.52	74.59	34.61	47.36	63.82

*Total Fe is expressed as FeO.

Table 2. *Trace element and REE compositions of the subset of the samples analysed by ICP-MS*

	Basic to intermediate volcanic rocks												Acidic volcanic rocks					Sheeted dyke rocks									Met. sole rocks		
Sample:	B-471	B-476	B-480	B-483	B-485	B-487	B-490	B-492	B-614	B-616	B-620	B-627	B-474	B-496	B-497	B-557	B-615	B-502	B-504	B-505	B-506	B-508	B-509	B-510	B-511	B-512	B-338	B-347	B-354
Pb	0.4	0.9	0.8	2.6	2.4	2.2	1.8	1.3	0.6	1.1	1.2	0.6	2.4	5.1	5.6	2.1	1.2	0.9	1.0	1.1	0.6	0.1	0.2	0.1	0.1	0.1	2.6	0.4	0.9
Zn	84	35	51	66	51	61	60	74	26	80	81	144	19	29	17	74	20	71	101	67	61	25	26	43	27	66	16	20	8
Ni	20.9	59.9	16.5	3.4	5.2	6.2	3.9	7	1	7.2	7.4	8.8	2.2	1	2.5	0.3	<	33.3	8.8	15	29.7	9.8	13.9	12.9	11.7	36.3	6.2	25.8	44
Ba	17.9	73.6	167	144	260	331	196	39.5	49.1	235	30.7	104	16.9	259	171	103	349	21.2	18.2	17.5	15.9	17.8	12.1	15	29.3	21.1	320	120	46.7
Co	33.4	24.2	19.4	15.5	19.3	20	20.2	28.9	21.7	13.4	20.9	19.9	1.1	4.3	3.3	4.6	4.4	41.2	35.2	37.9	39.9	41.9	41.4	36.1	39.6	40.3	31.8	46.4	49.8
Ga	18.9	14.8	15.9	17.8	16.2	17.8	19.1	14.7	16.2	17.2	16.1	19.3	13.1	18.7	16.1	13.4	19.6	18.4	21.4	22.6	16	19.3	20.1	20.7	17.7	18.2	19.5	15.4	9.3
Hf	2.4	1.5	2.5	3.1	2.3	2.1	2.2	1.6	2.7	2.8	2.4	1.7	4.3	4.6	3.9	3.3	4.2	2.8	3.1	2.9	1.7	3.5	3.8	3.9	3.2	2.4	1.7	1.1	0.8
Nb	1.2	1.3	3.1	2.5	2.6	2.5	2.6	1.1	1.2	1.3	1	1	2.5	14.4	14	1.3	15	1.9	2.3	1.8	0.7	2.1	2.6	2.7	2.4	1.4	2.2	0.7	0.9
Rb	4.4	5.8	6.7	30.2	32.1	41.4	16.5	3.2	31.8	69.5	15.8	73.4	<	99.1	92.3	39.9	97.8	<	<	<	1.1	<	<	0.8	2.3	0.7	31.8	9.8	4.4
Sr	346	296	508	297	976	350	365	234	125	50.6	63	50.7	52.5	206	149	50.6	80	180	80.9	254	309	179	87.5	132	183	164	322	199	115
Ta	<	<	0.1	0.2	0.3	<	0.2	<	<	<	<	<	0.2	0.9	1	<	1	0.2	0.1	0.1	<	0.2	0.2	0.2	0.2	0.1	0.2	<	<
Th	<	0.6	4	3.8	4.3	3.6	5	0.6	0.8	1.3	0.5	0.5	1	12.2	13.7	0.6	9.4	0.3	0.4	0.4	<	0.2	0.4	0.7	0.2	0.2	0.9	<	0.6
U	0.1	0.2	0.9	0.9	0.9	0.7	1.2	0.2	0.4	0.3	0.2	0.2	0.4	4.6	3.8	0.3	2.1	0.1	0.2	0.1	<	<	0.1	0.1	0.1	<	0.7	<	0.3
V	365	258	194	168	188	184	197	367	119	177	208	297	7	54	46	37	18	310	387	327	244	330	343	318	326	295	315	283	215
Zr	83.6	45.5	76.4	127	73.1	73.2	76.9	52.3	77.5	86.9	68.6	60.8	137	174	167	93.5	151	101	112	110	59.8	111	138	163	108	86.6	38	29.1	18.2
Y	36.7	20.1	21.6	20.8	19.9	24.1	23.2	24.3	33.2	32.3	39.2	25.2	45.2	27.3	23.6	36.7	38	39.3	41.8	40.1	28.5	46.3	52.6	58	45.5	37.9	31	25.6	12.4
La	3.8	4.6	17.5	14.6	13.4	15.6	15.8	6.1	3.9	3.9	4.8	3.5	8.5	30.8	29.2	4.8	28.5	4.8	4.9	4.9	2.2	4.8	5.9	6.6	4.7	3.4	6.8	1.6	5.5
Ce	10.9	11	33.5	27	26	29.8	32.9	13.8	10.2	10.8	12.6	9.8	21.7	55.9	53.8	13	53.6	13.3	14.7	14.4	6.6	14.3	18.3	19.9	14.5	10.9	17.9	5.5	11.3
Pr	1.89	1.59	3.73	3.11	3.07	3.45	3.98	2.02	1.58	1.75	1.86	1.49	2.97	5.44	5.23	1.98	5.73	2.15	2.27	2.26	1.25	2.26	2.97	3.14	2.3	1.81	2.78	1.02	1.36
Nd	11.6	8.8	18.4	15.5	16.6	19.2	18.6	11.4	9.7	9.9	11.5	9.5	16.9	22.2	21.7	11.7	25.1	12.6	15.6	13.9	8	14.8	17.2	18.7	14.1	12	15.8	6.9	8.1
Sm	3.4	2.2	3.6	2.8	3.5	3.6	3.6	3	2.9	3	3.6	2.5	4.3	3.9	3.6	3.3	5.4	3.7	4	4	2.8	4.5	5.2	5.9	4.6	3.9	3.8	2.4	2
Eu	1.38	0.8	0.97	1.09	1.1	1.15	1.11	1.1	1	0.91	1.29	0.74	1.07	0.98	0.83	1.04	1.31	1.45	1.48	1.6	0.98	1.66	1.81	1.86	1.63	1.36	1.36	0.96	0.62
Gd	4.63	2.68	3.44	3.18	3.15	4.14	3.65	3.55	4.62	4.09	4.55	3.38	4.94	3.38	3.18	4.8	5.64	5.25	5.67	5.56	3.81	5.78	6.93	8	5.93	5.19	4.49	3.33	1.99
Tb	0.9	0.53	0.58	0.52	0.55	0.62	0.62	0.64	0.72	0.73	0.83	0.59	1	0.62	0.59	0.8	0.87	1.02	1.04	0.99	0.7	1.25	1.22	1.48	1.06	0.94	0.8	0.62	0.37
Dy	5.93	3.03	3.53	3.11	3.27	3.99	3.58	4.3	5.27	5	5.75	4.2	6.29	4.27	3.81	5.56	5.73	6.49	7.66	6.56	4.55	7.55	8.79	9.18	7.35	5.98	4.77	4.08	2.04
Ho	1.33	0.7	0.79	0.7	0.76	0.87	0.81	0.85	1.12	1.12	1.36	1	1.63	0.92	0.84	1.26	1.33	1.4	1.55	1.37	1.07	1.57	1.77	1.96	1.64	1.28	1.06	0.96	0.46
Er	3.35	2	2.24	2.15	2.07	2.43	2.21	2.47	3.37	3.54	3.43	2.82	4.74	2.71	2.42	3.67	3.58	4.19	4.2	4.19	2.88	4.5	5.47	5.95	4.4	3.94	2.99	2.59	1.3
Tm	0.52	0.3	0.35	0.33	0.31	0.35	0.33	0.42	0.5	0.56	0.6	0.43	0.74	0.41	0.39	0.6	0.61	0.64	0.66	0.57	0.45	0.72	0.82	0.88	0.73	0.53	0.41	0.32	0.2
Yb	3.61	2.4	2.53	2.4	2.14	2.42	2.55	2.65	3.71	3.71	3.77	3.09	5.43	2.8	3.06	3.96	3.95	3.74	4.17	3.65	2.75	4.35	5.71	5.7	4.3	3.43	3.48	2.76	1.32
Lu	0.48	0.34	0.35	0.31	0.29	0.35	0.35	0.37	0.56	0.55	0.57	0.46	0.79	0.45	0.43	0.59	0.65	0.57	0.61	0.55	0.42	0.65	0.79	0.84	0.67	0.56	0.52	0.33	0.19

<, below detection limit.

Table 3. *Representative analyses of major elements for olivines and plagioclases in the cumulate rocks*

	Gabbroic cumulates[1]							Gabbroic cumulates[2]									
Sample:	B406-1c	B406-1r	B406-2c	B406-2r	B406-3c	B406-4c	B406-5c	Sample	B406-2c	B406-4c	B406-6c	B406-4c	B326-3c	B326-6c	B326-7c	B341-1c	B341-4c	B341-5c	B341-7c
SiO_2	38.79	38.88	38.96	38.69	39.10	39.01	38.82	SiO_2	44.95	44.42	44.96	45.45	48.31	54.89	51.88	57.38	54.64	56.78	56.46
TiO_2	0.01	0.00	0.01	0.00	0.02	0.00	0.00	TiO_2	0.00	0.00	0.00	0.00	0.02	0.00	0.00	0.03	0.01	0.02	0.01
Al_2O_3	0.01	0.00	0.00	0.01	0.01	0.01	0.01	Al_2O_3	35.06	34.93	34.58	33.93	32.59	28.45	30.28	26.65	28.59	27.43	27.79
Cr_2O_3	0.00	0.00	0.00	0.00	0.05	0.00	0.00	FeO*	0.28	0.19	0.27	0.28	0.31	0.20	0.21	0.13	0.07	0.11	0.14
FeO*	22.79	22.24	22.51	23.08	21.60	22.49	22.09	MnO	0.01	0.00	0.02	0.01	0.03	0.02	0.00	0.02	0.00	0.00	0.00
MnO	0.45	0.41	0.41	0.41	0.45	0.41	0.39	MgO	0.01	0.03	0.01	0.01	0.00	0.00	0.02	0.00	0.00	0.00	0.01
MgO	37.71	38.52	38.40	37.99	38.83	38.06	38.72	CaO	18.89	18.66	18.52	18.39	15.27	10.51	12.69	9.38	11.49	9.79	10.32
NiO	0.03	0.03	0.00	0.00	0.02	0.01	0.01	Na_2O	0.60	0.82	0.75	0.85	2.37	5.13	3.86	6.04	4.77	5.81	5.55
CaO	0.01	0.01	0.01	0.02	0.03	0.01	0.03	K_2O	0.01	0.00	0.01	0.01	0.09	0.30	0.20	0.12	0.08	0.11	0.11
Total	99.80	100.10	100.300	100.20	100.10	99.99	100.07	Total	99.81	99.04	99.11	98.92	98.99	99.49	99.14	99.75	99.64	100.06	100.40
Si	1.01	1.01	1.01	1.01	1.01	1.01	1.01	Si	2.08	2.07	2.10	2.12	2.23	2.49	2.38	2.59	2.48	2.56	2.54
Ti	0.00	0.00	0.00	0.00	0.00	0.00	0.00	Al(IV)	0.92	0.93	0.90	0.88	0.77	0.51	0.62	0.41	0.52	0.44	0.46
Al	0.00	0.00	0.00	0.00	0.00	0.00	0.00	Al(VI)	1.00	0.99	1.00	0.99	1.01	1.01	1.01	1.01	1.01	1.01	1.01
Cr	0.00	0.00	0.00	0.00	0.00	0.00	0.00	Ti	0.00	0.00	0.00	0.00	0.00	0.00	0.00	0.00	0.00	0.00	0.00
Fe	0.50	0.48	0.49	0.50	0.47	0.49	0.48	Fe	0.01	0.01	0.01	0.01	0.01	0.01	0.01	0.00	0.00	0.00	0.01
Mn	0.01	0.01	0.01	0.01	0.01	0.01	0.01	Mn	0.00	0.00	0.00	0.00	0.00	0.00	0.00	0.00	0.00	0.00	0.00
Mg	1.47	1.49	1.48	1.47	1.50	1.47	1.50	Mg	0.00	0.00	0.00	0.00	0.00	0.00	0.00	0.00	0.00	0.00	0.00
Ni	0.00	0.00	0.00	0.00	0.00	0.00	0.00	Ca	0.94	0.93	0.92	0.92	0.76	0.51	0.62	0.45	0.56	0.47	0.50
Ca	0.00	0.00	0.00	0.00	0.00	0.00	0.00	Na	0.05	0.07	0.07	0.08	0.21	0.45	0.34	0.53	0.42	0.51	0.48
Total	2.99	2.99	2.99	2.99	2.99	2.99	2.99	K	0.00	0.00	0.00	0.00	0.01	0.02	0.01	0.01	0.00	0.01	0.01
								Total	5.00	5.00	5.00	5.00	5.00	5.00	5.00	5.00	5.00	5.00	5.00
Fo	74.69	75.53	75.26	74.59	76.22	75.11	75.76												
Fa	25.31	24.47	24.74	25.41	23.78	24.89	24.24	Or	0.08	0.00	0.03	0.04	0.53	1.76	1.20	0.72	0.47	0.67	0.66
								Ab	5.42	7.36	6.81	7.73	21.82	46.07	35.07	53.42	42.68	51.44	48.99
								An	94.50	92.64	93.16	92.23	77.64	52.17	63.72	45.87	56.85	47.89	50.34

[1]Number of ions on the basis of four (O).
[2]Number of ions on the basis of 16 (O).
*Total Fe is expressed as FeO.

Table 4. *Representative analyses of major elements for clino- and ortho-pyroxenes in the cumulate rocks*

	Clinopyroxene														Orthopyroxene				
	Gabbronorite						Olivine gabbro		Gabbronorite						Olivine gabbro				
Sample:	B326-2c	B326-3c	B326-9c	B326-10c	B403-3c	B403-4c	B406-3c	B406-4c	B326-1c	B326-4c	B326-5c	B326-6c	B326-13c	B326-14c	B406-1c	B406-2c	B406-5c	B406-6c	B406-7c
SiO_2	52.14	52.86	52.23	51.9	49.08	49.84	60.46	57.33	52.28	52.52	52.72	52.42	52.84	52.98	55.06	54.55	54.24	54.52	54.35
Al_2O_3	1.62	1.39	1.64	1.67	7.35	7.15	0.07	0.14	0.89	0.81	0.73	0.91	0.87	0.86	2.14	2.20	2.58	2.62	2.34
TiO_2	0.28	0.24	0.37	0.35	1.22	1.04	0.02	0.01	0.21	0.17	0.14	0.20	0.15	0.17	0.11	0.11	0.07	0.05	0.07
FeO*	9.61	9.29	9.65	9.61	12.57	12.15	2.08	5.13	24.00	23.75	23.66	23.83	22.38	22.09	14.06	13.98	13.96	14.18	14.48
MnO	0.53	0.55	0.52	0.56	0.26	0.25	0.18	0.08	1.07	1.24	1.23	1.24	1.17	1.08	0.46	0.35	0.38	0.42	0.43
MgO	13.85	13.85	13.62	13.78	15.03	15.62	23.99	25.67	20.89	20.70	20.78	20.63	21.81	21.91	28.27	28.16	28.05	27.61	27.66
Cr_2O_3	0.01	0.02	0.00	0	0.01	0.01	0.00	0.00	0.00	0.02	0.00	0.00	0.02	0.00	0.01	0.00	0.03	0.01	0.00
CaO	20.79	21.18	21.12	20.8	11.30	11.52	12.89	11.33	0.96	1.00	0.87	0.91	0.95	1.12	0.38	0.35	0.36	0.27	0.37
Na_2O	0.29	0.30	0.32	0.34	0.94	0.81	0.00	0.02	0.00	0.00	0.01	0.00	0.00	0.00	0.00	0.00	0.01	0.01	0.00
K_2O	0.01	0.00	0.00	0	0.45	0.44	0.01	0.00	0.00	0.01	0.01	0.00	0.00	0.01	0.00	0.00	0.01	0.01	0.01
Total	99.14	99.68	99.46	99	98.21	98.82	99.70	99.70	100.30	100.21	100.16	100.14	100.18	100.23	100.49	99.70	99.70	99.70	99.70
Si	1.96	1.98	1.96	1.96	1.85	1.86	2.16	2.04	1.96	1.97	1.98	1.97	1.97	1.97	1.96	1.96	1.94	1.96	1.95
Al(IV)	0.04	0.02	0.04	0.04	0.15	0.14	−0.16	−0.04	0.04	0.03	0.02	0.03	0.03	0.03	0.04	0.04	0.06	0.04	0.05
Al(VI)	0.03	0.04	0.03	0.03	0.17	0.17	0.16	0.05	0.00	0.01	0.01	0.01	0.01	0.01	0.05	0.05	0.05	0.07	0.05
Ti	0.01	0.01	0.01	0.01	0.03	0.03	0.00	0.00	0.01	0.00	0.00	0.01	0.00	0.00	0.00	0.00	0.00	0.00	0.00
Fe^{3+}	0.01	−0.01	0.01	0.02	0.00	−0.01	−0.32	−0.09	0.03	0.01	0.00	0.00	0.01	0.01	−0.02	−0.01	0.00	−0.03	−0.01
Fe^{2+}	0.29	0.30	0.30	0.28	0.39	0.39	0.38	0.24	0.73	0.74	0.74	0.74	0.69	0.68	0.43	0.43	0.42	0.46	0.45
Mn	0.02	0.02	0.02	0.02	0.01	0.01	0.01	0.00	0.03	0.04	0.04	0.04	0.04	0.03	0.01	0.01	0.01	0.01	0.01
Mg	0.78	0.77	0.76	0.77	0.84	0.87	1.28	1.36	1.17	1.16	1.16	1.16	1.21	1.22	1.50	1.51	1.50	1.48	1.48
Cr	0.00	0.00	0.00	0	0.00	0.00	0.00	0.00	0.00	0.00	0.00	0.00	0.00	0.00	0.00	0.00	0.00	0.00	0.00
Ca	0.84	0.85	0.85	0.84	0.46	0.46	0.49	0.43	0.04	0.04	0.04	0.04	0.04	0.04	0.01	0.01	0.01	0.01	0.01
Na	0.02	0.02	0.02	0.02	0.07	0.06	0.00	0.00	0.00	0.00	0.00	0.00	0.00	0.00	0.00	0.00	0.00	0.00	0.00
K	0.00	0.00	0.00	0	0.02	0.02	0.00	0.00	0.00	0.00	0.00	0.00	0.00	0.00	0.00	0.00	0.00	0.00	0.00
Total	4.00	4.00	4.00	4	4.00	4.00	4.00	4.00	4.00	4.00	4.00	4.00	4.00	4.00	4.00	4.00	4.00	4.00	4.00
En	40.16	40.03	39.47	40.02	49.53	50.62	69.49	69.89	58.60	58.40	58.74	58.35	61.07	61.34	77.05	77.25	77.15	76.69	76.23
Fs	16.51	15.97	16.54	16.57	23.72	22.54	3.68	7.95	39.47	39.57	39.49	39.80	37.01	36.41	22.20	22.06	22.14	22.76	23.05
Wo	43.33	44.00	43.99	43.41	26.75	26.84	26.84	22.16	1.93	2.03	1.77	1.85	1.92	2.26	0.75	0.69	0.71	0.55	0.72
Mg-no.	71.97	72.65	71.56	71.89	68.07	69.63	95.36	89.92	60.81	60.84	61.02	60.68	63.46	63.88	78.20	78.21	78.17	77.64	77.31

Number of ions on the basis of six (O).
*Total Fe is expressed as FeO.

Table 5. *Representative analyses of major elements for amphiboles in the cumulate and metamorphic sole rocks*

	Metamorphic sole rocks							Cumulate rocks									
	Amphibolites							Amphibole gabbro		Gabbronorite					Olivine gabbro		
Sample:	B338-3c	B338-4c	B338-4c	B347-3c	B347-7c	B354-1c	B354-4c	B341-1c	B341-2c	B326-1c	B326-6c	B403-3c	B403-6c	B403-11c	B406-1c	B406-3c	B406-4c
SiO_2	46.05	46.97	43.15	49.01	48.44	45.16	51.28	45.58	47.10	46.24	49.83	46.77	48.79	44.89	44.86	45.55	44.77
TiO_2	1.41	0.98	0.80	1.35	1.39	0.78	0.34	1.27	1.27	1.54	1.11	1.33	1.13	1.81	1.27	0.74	0.94
Al_2O_3	9.64	9.07	12.75	7.62	8.15	11.06	5.58	10.50	8.90	8.24	6.26	9.28	7.57	10.18	13.68	12.64	13.61
Cr_2O_3	0.00	0.00	0.00	0.03	0.02	0.16	0.73	0.02	0.00	0.01	0.00	0.00	0.03	0.00	0.02	0.01	0.02
FeO	14.73	15.45	17.08	12.53	12.86	10.36	7.72	15.60	15.30	14.08	12.57	12.71	11.95	13.61	8.63	8.74	8.47
MnO	0.39	0.31	0.28	0.24	0.26	0.20	0.17	0.53	0.53	0.36	0.29	0.26	0.23	0.23	0.15	0.18	0.12
MgO	12.11	11.88	10.11	14.32	13.90	14.70	17.63	11.61	12.58	13.55	15.18	14.19	15.19	13.41	15.75	16.39	15.93
CaO	11.43	11.59	11.28	11.77	11.85	12.25	12.50	11.11	10.78	11.02	11.20	11.26	11.51	11.41	11.59	11.54	11.59
Na_2O	1.11	1.03	1.36	1.20	1.22	1.41	0.58	1.22	1.20	1.05	0.76	0.99	0.84	1.27	1.84	1.73	1.88
K_2O	0.31	0.23	0.72	0.13	0.18	0.44	0.23	0.58	0.48	0.69	0.46	0.62	0.46	0.70	0.26	0.29	0.26
Total	97.18	97.51	97.53	98.18	98.28	96.53	96.76	98.02	98.14	96.78	97.66	97.41	97.69	97.53	98.04	97.81	97.59
Si	6.71	6.84	6.35	7.00	6.94	6.55	7.28	6.60	6.76	6.72	7.08	6.70	6.94	6.50	6.29	6.37	6.29
Al (IV)	1.29	1.16	1.65	1.00	1.06	1.45	0.72	1.40	1.24	1.28	0.92	1.30	1.06	1.50	1.71	1.63	1.71
Al (VI)	0.37	0.39	0.56	0.28	0.31	0.44	0.21	0.40	0.27	0.14	0.13	0.27	0.21	0.23	0.55	0.46	0.55
Fe^{+3}	0.67	0.60	0.84	0.48	0.45	0.54	0.35	0.82	0.95	0.94	0.84	0.89	0.79	0.85	0.87	1.02	0.91
Ti	0.15	0.11	0.09	0.14	0.15	0.09	0.04	0.14	0.14	0.17	0.12	0.14	0.12	0.20	0.13	0.08	0.10
Cr	0.00	0.00	0.00	0.00	0.00	0.02	0.08	0.00	0.00	0.00	0.00	0.00	0.00	0.00	0.00	0.00	0.00
Fe^{+2}	1.13	1.28	1.26	1.02	1.09	0.71	0.57	1.07	0.88	0.77	0.65	0.63	0.63	0.80	0.14	0.00	0.09
Mn	0.05	0.04	0.04	0.03	0.03	0.02	0.02	0.07	0.06	0.04	0.04	0.03	0.03	0.03	0.02	0.02	0.01
Mg	2.63	2.58	2.22	3.05	2.97	3.18	3.73	2.51	2.69	2.94	3.22	3.03	3.22	2.89	3.29	3.42	3.34
Ca	1.78	1.81	1.78	1.80	1.82	1.90	1.90	1.72	1.66	1.72	1.71	1.73	1.75	1.77	1.74	1.73	1.75
Na	0.31	0.29	0.39	0.33	0.34	0.40	0.16	0.34	0.33	0.30	0.21	0.28	0.23	0.36	0.50	0.47	0.51
K	0.06	0.04	0.13	0.02	0.03	0.08	0.04	0.11	0.09	0.13	0.08	0.11	0.08	0.13	0.05	0.05	0.05
Total	15.16	15.14	15.30	15.15	15.19	15.38	15.10	15.17	15.08	15.14	15.00	15.12	15.07	15.26	15.29	15.25	15.31

Number of ions is on the basis of 23 (O).
*Total Fe is expressed as FeO

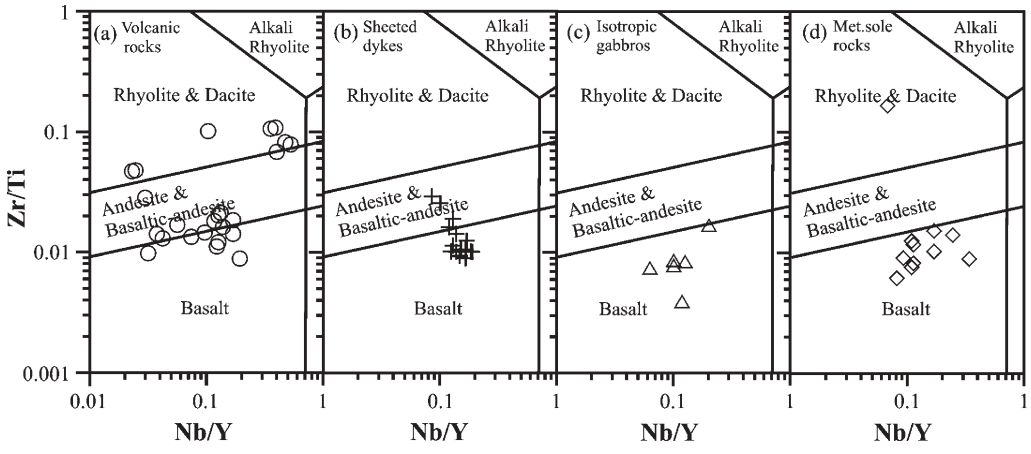

Fig. 6. Rock classification diagrams based on Nb/Y v. Zr/Ti (Pearce 1996) for the Kömürhan ophiolite rocks.

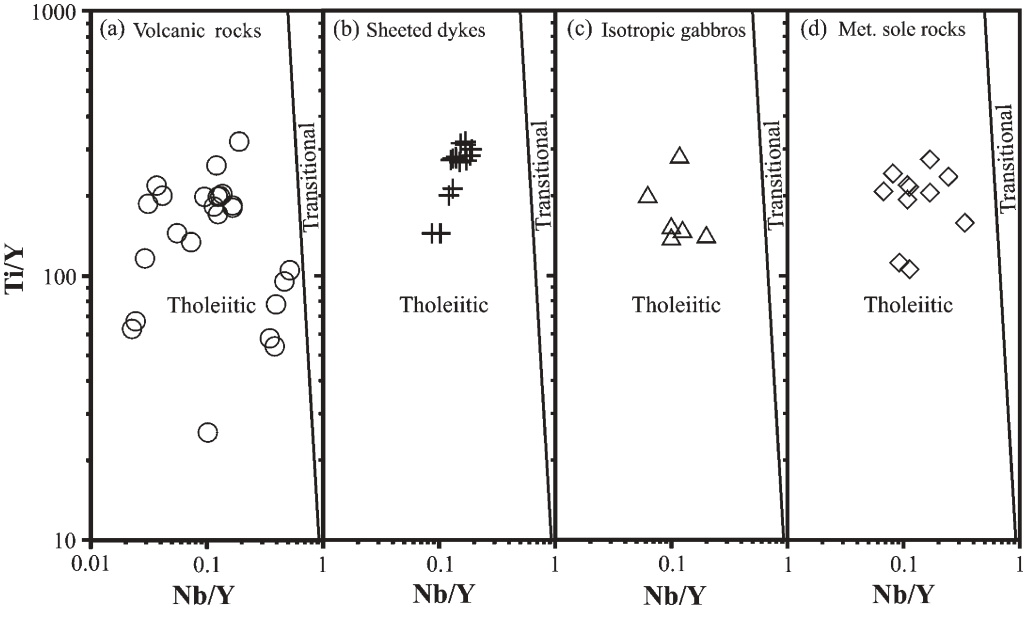

Fig. 7. Nb/Y v. Ti/Y diagrams showing tholeiitic nature of the Kömürhan ophiolite rocks (Pearce 1982).

(Fig. 7). To exhibit the chemical relationships of the Kömürhan ophiolite rocks, several diagrams based on immobile elements are presented in Figure 8. In the TiO_2 v. Zr diagram (Fig. 8a), the volcanic rocks define a decreasing trend with increasing Zr from basic (1.43%) to acidic (0.21%) rocks, suggesting magnetite or titanomagnetite crystallization in the more evolved rocks. By contrast, the sheeted dyke rocks have a high content TiO_2 (1.20–2.69%) compared with the volcanic rocks and the metamorphic sole rocks (0.16–1.28%). The Y and FeO*/MgO ratios of the rocks, plotted against Zr in Figure 8b and c show a positive correlation and coherent trends. By contrast, a decreasing Y content in some of the acidic volcanic rocks may be caused by amphibole fractionation. The chemical features displayed suggest that the volcanic rocks, sheeted dykes and the protolith of the metamorphic sole rocks represent a differentiated co-magmatic tholeiitic suite, exhibiting similar fractionation trends.

Representative analyses of major and trace element contents of the cumulate rocks and the

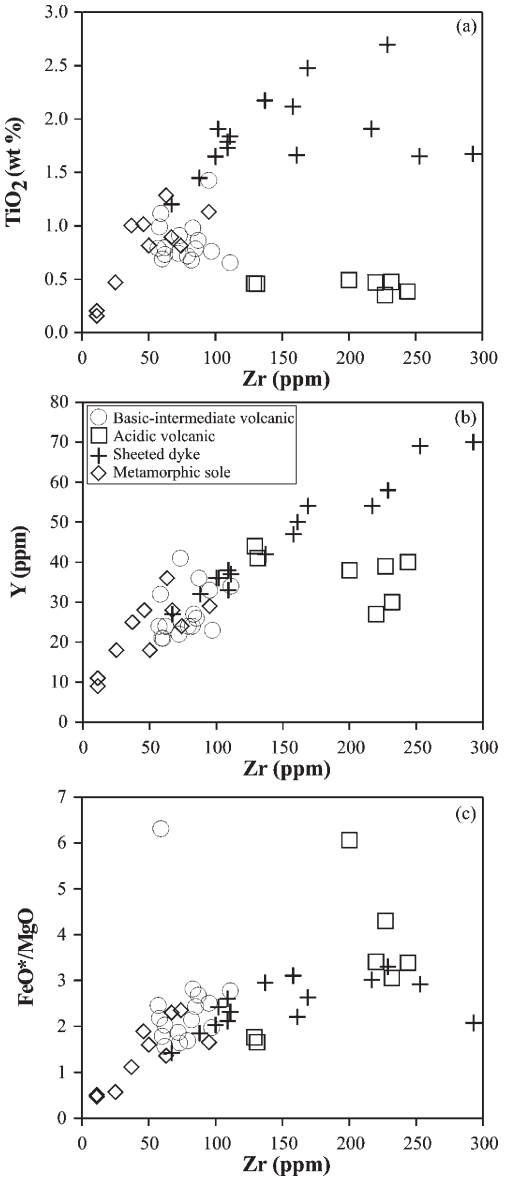

Fig. 8. Major and trace element variations against Zr for the Kömürhan ophiolite rocks.

isotropic gabbros are presented in Table 1. Loss on ignition (LOI) values are up to 3.05% in the mafic cumulates and 6.97% in one ultramafic cumulate rock sample (Table 1), indicating variable amount of serpentinization or alteration. The Al_2O_3, CaO, Ni and Cr contents of the isotropic gabbro and the ultramafic to mafic cumulate rocks are plotted against Mg-number ($100 \times MgO/(MgO + FeO)$) as an indication of the degree of differentiation (Fig. 9). The CaO content is 6.09 wt% in wehrlite and ranges from 20.9 to 9.44 wt% in gabbroic rocks, and from 15.59 to 8.72 wt% in the isotropic gabbros; it is negatively correlated with MgO (Fig. 9b). The Al_2O_3 content, which is also negatively correlated with increasing MgO, shows lower values in wehrlite (5.73 wt%), but higher values in cumulate gabbros (from 27.57 to 13.39 wt%) and in isotropic gabbros (from 18.39 to 14.81 wt%) (Fig. 9a). The high CaO and Al_2O_3 contents in the gabbroic rocks are an indication of the presence of plagioclase (An_{95-45}). Ni and Cr contents decrease markedly from high values in wehrlite (633 ppm for Ni and 1081 ppm for Cr) to much lower values in plagioclase-rich gabbros (from 306 to 3 ppm for Ni and from 1483 to 4 ppm for Cr), consistent with the fractionation of olivine, spinel and clinopyroxene (Fig. 9c and d).

The REE patterns of the volcanic, sheeted dyke and metamorphic sole rocks are presented in Figure 10. The basic to intermediate volcanic rocks exhibit (1) flat [$(La/Yb)_N = 1.65–0.75$] and (2) marked light rare earth element (LREE) enrichments with respect to heavy rare earth element (HREE) ($(La/Yb)_N = 4.96–4.36$). The acidic volcanic rocks also exhibit similar REE patterns; one group has a flat pattern ($(La/Yb)_N = 1.12–0.87$) and a second has an LREE-enriched pattern ($(La/Yb)_N = 7.89–5.18$) (Fig. 10). These samples exhibit a slight Eu negative anomaly, as a consequence of the removal of feldspar by fractional crystallization or the partial melting of a source material in which feldspar is retained in the source (Rollinson 1993). The sheeted dyke complex generally exhibits slightly LREE-depleted to flat ($(La/Yb)_N = 0.96–0.57$) REE patterns with an overall enrichment of 10–30 times chondritic values (Fig. 10). The metamorphic sole rocks display slightly LREE-enriched ($(La/Yb)_N = 2.99–1.40$) to LREE-depleted ($(La/Yb)_N = 0.42$) patterns (Fig. 10). The enrichment of the LREE is commonly interpreted as a consequence of mantle source enrichment by subduction-derived components (Floyd *et al.* 1991; Bortolotti *et al.* 2004). Flat to LREE-enriched patterns are typically found in island-arc tholeiites (Pearce 1982; Peate *et al.* 1997) and suprasubduction-zone type ophiolites of the eastern Mediterranean (Desmons *et al.* 1980; Searle *et al.* 1980; Alabaster *et al.* 1982; Pearce *et al.* 1984; Parlak 1996; Yalınız *et al.* 1996, 2000; Parlak *et al.* 2000; Al-Riyami *et al.* 2002).

Figure 11 presents normal mid-ocean ridge basalt (N-MORB)-normalized spider diagrams of the volcanic, sheeted dyke and metamorphic sole rocks of the Kömürhan ophiolite. Some general features include (1) enrichment in large ion lithophile elements (LILE; Rb, Ba, Th, K)

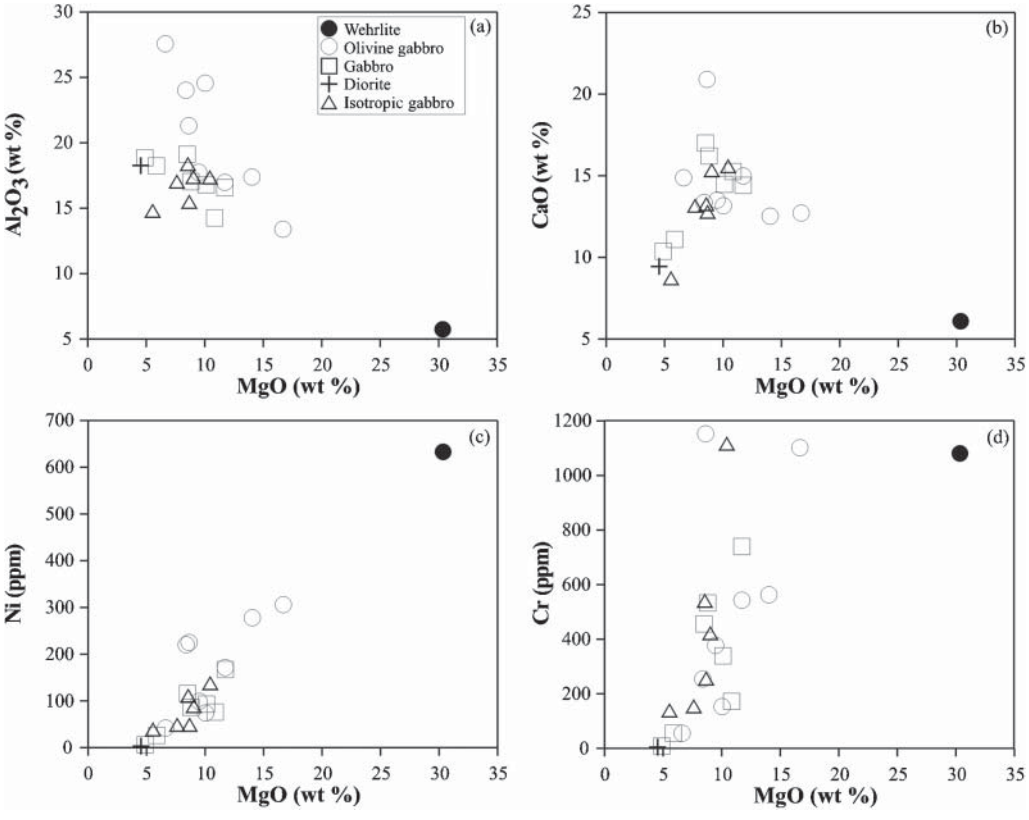

Fig. 9. Selected major and trace element variations for the gabbroic and wehrlitic rocks.

elements; (2) depletion in Nb; (3) flat patterns of high field strength elements (HFSE) relative to N-MORB (Fig. 11). Th enrichment (together with the LREE) and Nb–Ta depletion are features of subduction-related volcanic rocks (Wood *et al.* 1979; Pearce 1983; Arculus & Powel 1986; Yogodzinski *et al.* 1993; Wallin & Metcalf 1998). The Th enrichment and Nb depletion of the Kömürhan ophiolite rocks imply their formation in a subduction-related tectonic setting.

Nb/Th ratio v. Y discriminates between subduction and non-subduction settings based on Nb enrichment or depletion (Jenner *et al.* 1991). The volcanic rocks, sheeted dykes and metamorphic sole rocks of the Kömürhan ophiolite plot within the arc-related field (Fig. 12a). The Th/Yb v. Ta/Yb plot discriminates between depleted mantle (MORB) and enriched mantle (intraplate) sources (Pearce 1982). Addition of a subduction component from slab-derived fluids or melts results in an increase in Th/Yb in the mantle source, as shown by the arrow (Fig. 12b). On this diagram, all the rocks plot within the volcanic arc field. The Th–Hf–Nb triangular diagram (Wood *et al.* 1979), and the Zr–Nb–Y triangular diagram (Meschede 1986) discriminate volcanic rocks erupted in different geotectonic settings. The volcanic rocks, sheeted dykes, isotropic gabbros and metamorphic sole rocks from the Kömürhan ophiolite plot within the subduction-related field (Fig. 13a and b).

Mineral chemistry

Cumulus olivine (unzoned) analyses from the gabbroic cumulate rocks are presented in Table 3. Their Fo contents range from 76.2 to 73.9. NiO content ranges from zero to 0.06% (Table 3). Representative plagioclase analyses from the mafic cumulate rocks are presented in Table 3. The plagioclase has a very wide compositional range: from $An_{94.8}$ to $An_{92.2}$ in olivine gabbro, from $An_{77.8}$ to $An_{52.2}$ in gabbronorites, and from $An_{56.9}$ to $An_{43.4}$ in amphibole gabbro (Table 3). The basic to evolved rock types in the cumulates have resulted in variable An contents. Plagioclases in the amphibole gabbro exhibit both reverse and normal zoning, whereas plagioclases

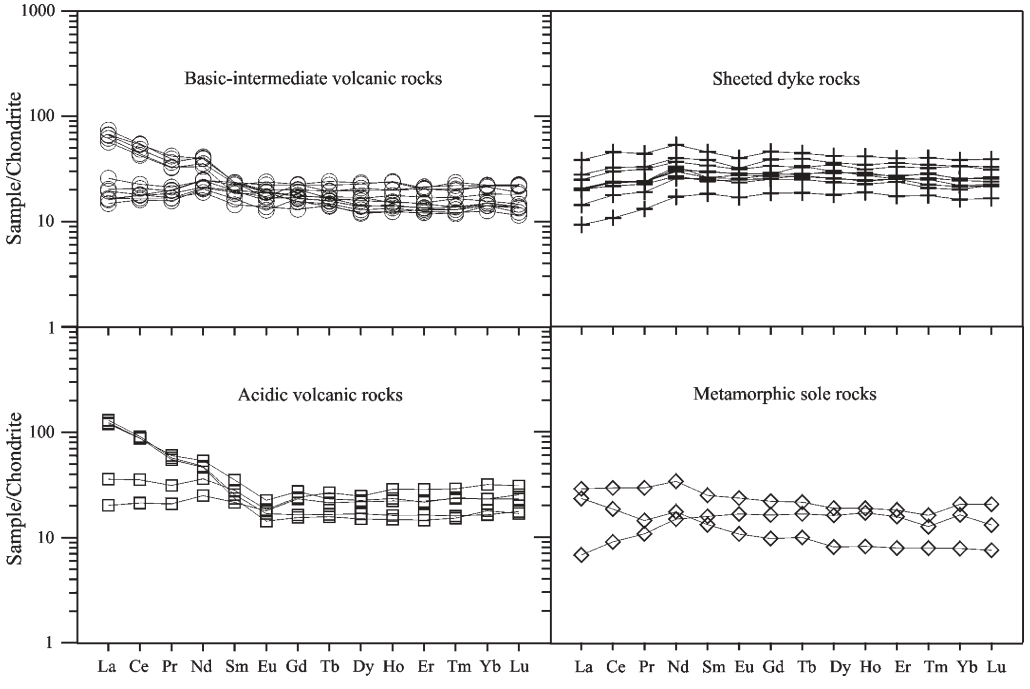

Fig. 10. REE diagrams of the Kömürhan ophiolite rocks (normalizing values are from Sun & McDonough 1989).

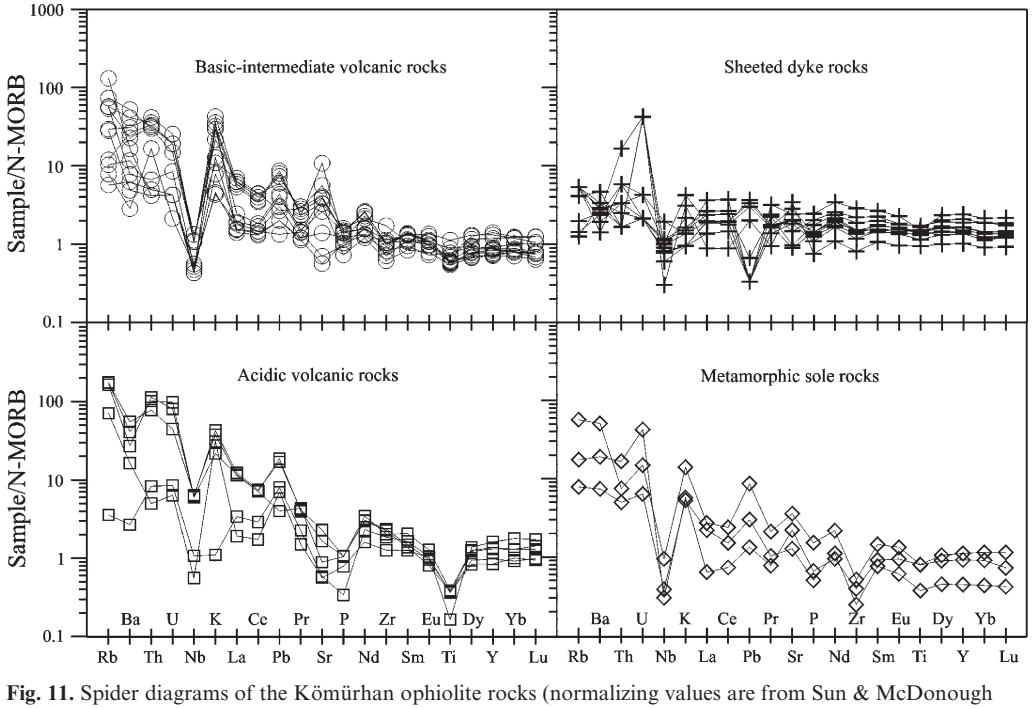

Fig. 11. Spider diagrams of the Kömürhan ophiolite rocks (normalizing values are from Sun & McDonough 1989).

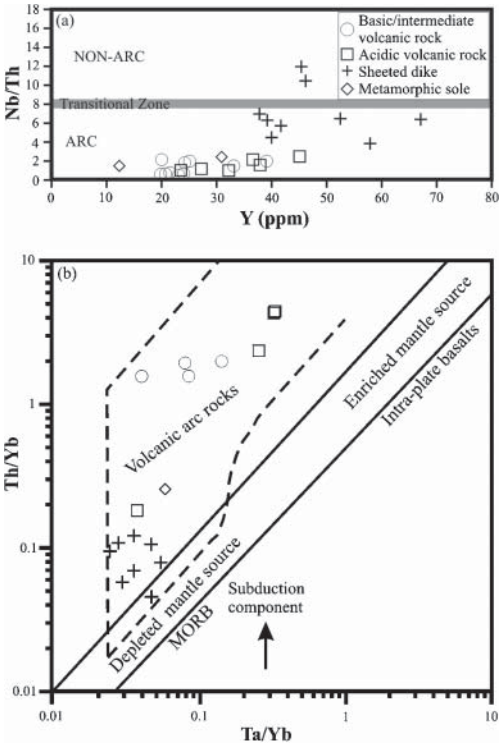

Fig. 12. (**a**) Nb/Th v. Y diagram (after Jenner *et al.* 1991) and (**b**) Ta/Yb v. Th/Yb diagram (after Pearce 1982), showing the typically arc-like signature of the Kömürhan ophiolite rocks.

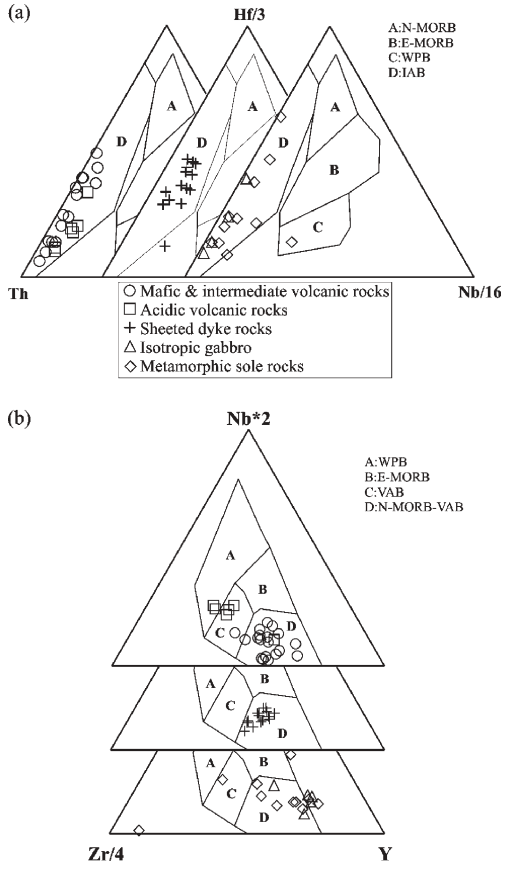

Fig. 13. (**a**) Th–Hf–Nb (after Wood *et al.* 1979) and (**b**) Zr–Nb–Y (after Meschede 1986) tectonomagmatic discrimination diagrams for the rocks of the Kömürhan ophiolite. N-MORB, normal mid-ocean ridge basalt; E-MORB, enriched MORB; WPB, within-a-plate basalt; IAB, island-arc basalt; VAB, volcanic arc basalt.

in more basic cumulate rocks (gabbronorite and olivine gabbro) are unzoned. Clinopyroxene analyses from the gabbroic cumulate rocks are presented in Table 4. In terms of quadrilateral components, the cumulus clinopyroxene composition is $En_{50.6–39.5}$ $Fs_{23.7–14.6}Wo_{44.9–26.8}$ in gabbronorite, and $En_{69.9–69.5}Fs_{8.0–3.7}Wo_{26.8–22.2}$ in olivine gabbro. The Mg-number of the clinopyroxene ranges from 74 to 68 in gabbronorite, from 95 to 90 in olivine gabbro (Table 4). Representative orthopyroxene analyses from the mafic cumulate rocks are presented in Table 4. The orthopyroxene composition is $En_{61.3–57.9}Fs_{40.4–36.4}Wo_{2.3–1.3}$ in the gabbronorite, and $En_{77.3–76.2}Fs_{23.1–22.1}Wo_{0.8–0.6}$ in olivine gabbro. The Mg-number of the orthopyroxene ranges from 63.9 to 60.1 in the gabbronorite, and from 78.2 to 77.3 in the olivine gabbro. Representative analyses of amphiboles from the cumulate rocks are presented in Table 5. The amphiboles in the amphibole gabbro rocks are primary and represented by magnesio-hornblende, whereas the amphiboles in the gabbronorite and olivine gabbro are secondary, derived from alteration of pyroxenes and represented by magnesio-hornblende in gabbronorite and tschermakite in olivine gabbro (Table 5). The Mg-number of the amphiboles is 56.4–59.4 for amphibole gabbros, 70.3–63.7 for gabbronorites, and 77.9–75.9 for olivine gabbro.

Covariation of An content of plagioclase v. Mg-number of orthopyroxene and olivine for the gabbroic rocks is shown in Figure 14a and b, together with results from the Troodos (Hébert & Laurent 1990), Mersin (Parlak *et al.* 1996), Pozantı–Karsantı (Parlak *et al.* 2000) and Kızıldağ (Bağcı *et al.* 2006) ophiolites, and other comparable units from well-documented tectonic settings. The mineral compositions of the gabbroic rocks from the Kömürhan ophiolite show

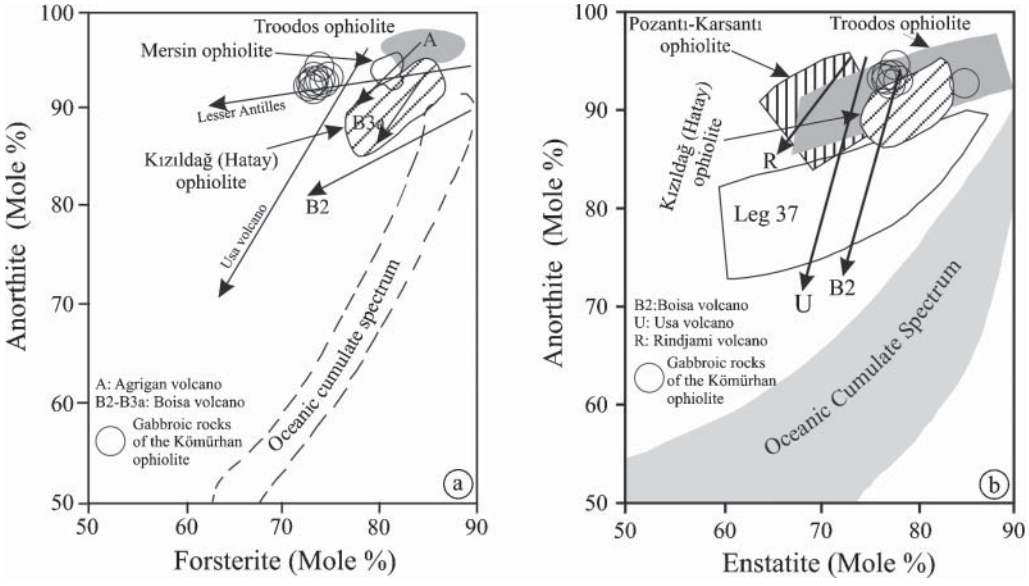

Fig. 14. (**a**) Anorthite content in plagioclase (mol%) v. Fo (mol%) content in olivine. (**b**) Anorthite content in plagioclase (mol%) v. enstatite content in orthopyroxene (mol%) for the Kömürhan ophiolite. The Troodos ophiolite trend is from Hébert & Laurent (1990). The Mersin ophiolite trend is from Parlak *et al.* (1996). The Pozantı–Karsantı ophiolite trend is from Parlak *et al.* (2000). The Kızıldağ ophiolite trend is from Bağcı *et al*. (2006). R, Rindjami volcano (Foden 1983); B2, B3a, Boisa volcano (Gust & Johnson 1981); U, Usa volcano (Fujimaki 1986); A, Agrigan volcano (Stern 1979); Data for Lesser Antilles are from Arculus & Wills (1980).

a close similarity to SSZ-type ophiolites of the eastern Mediterranean region and known island-arc settings (Stern 1979; Arculus & Wills 1980; Gust & Johnson 1981; Fujimaki 1986).

Discussion

The most important tectonomagmatic–stratigraphic units of SE Anatolia in the Late Cretaceous were (1) metamorphic massifs (i.e. Malatya–Keban platform), (2) ophiolites (i.e. Göksun, İspendere, Kömürhan and Guleman), (3) volcanic arc units (i.e. Yüksekova–Elazığ magmatics units); (4) granitic rocks (i.e. Baskil). The SE Anatolian orogenic evolution involved progressive relative (southerly) movement of the nappes towards the Arabian plate during Late Cretaceous–Miocene time (Yıldırım & Yılmaz 1991; Yılmaz 1993; Yılmaz *et al.* 1993; Robertson *et al*. 2006, 2007). The Malatya–Keban platform, belonging to the upper part of the nappe zone of the SE Anatolian orogen (Yılmaz 1993), was amalgamated with the SSZ-type ophiolites (Göksun–Kömürhan–İspendere–Guleman) and their arc-related volcanic succession (Yüksekova complex–Elazığ magmatic rocks) around 88–85 Ma (Parlak, 2006; Robertson *et al*. 2006, 2007).

The nature of the volcano-sedimentary units interbedded with the lavas, the major and trace element geochemistry of the volcanic rocks, as well as their wide compositional range (from basalt to rhyodacite) suggest that this assemblage represents the upper levels of an intra-oceanic volcanic arc formed above of north-dipping subduction zone during Late Cretaceous time. A similar volcano-sedimentary rock association has been reported from the same belt, notably the Göksun (N Berit) ophiolite (Parlak *et al.* 2004; Robertson *et al*. 2006) and Late Cretaceous arc-related rocks around Elazığ (Bölücek *et al.* 2004; Robertson *et al*. 2007). The sheeted dyke and isotropic gabbroic rocks in the Kömürhan ophiolite are tholeiitic in character (Nb/Y = 0.2–0.06). The REE patterns, multi-element and tectonomagmatic discrimination diagrams suggest their formation in a subduction-related environment. The major and trace element geochemistry of the cumulate rocks is similar to that observed in a modern island-arc tholeiite (IAT) sequence. Crystallization of calcic plagioclases in olivine gabbros and amphibole is suggestive of hydrous conditions during magma differentiation. The presence of intercumulus water in the cumulate rocks (Arculus & Wills 1980) may be responsible for the reverse zoning

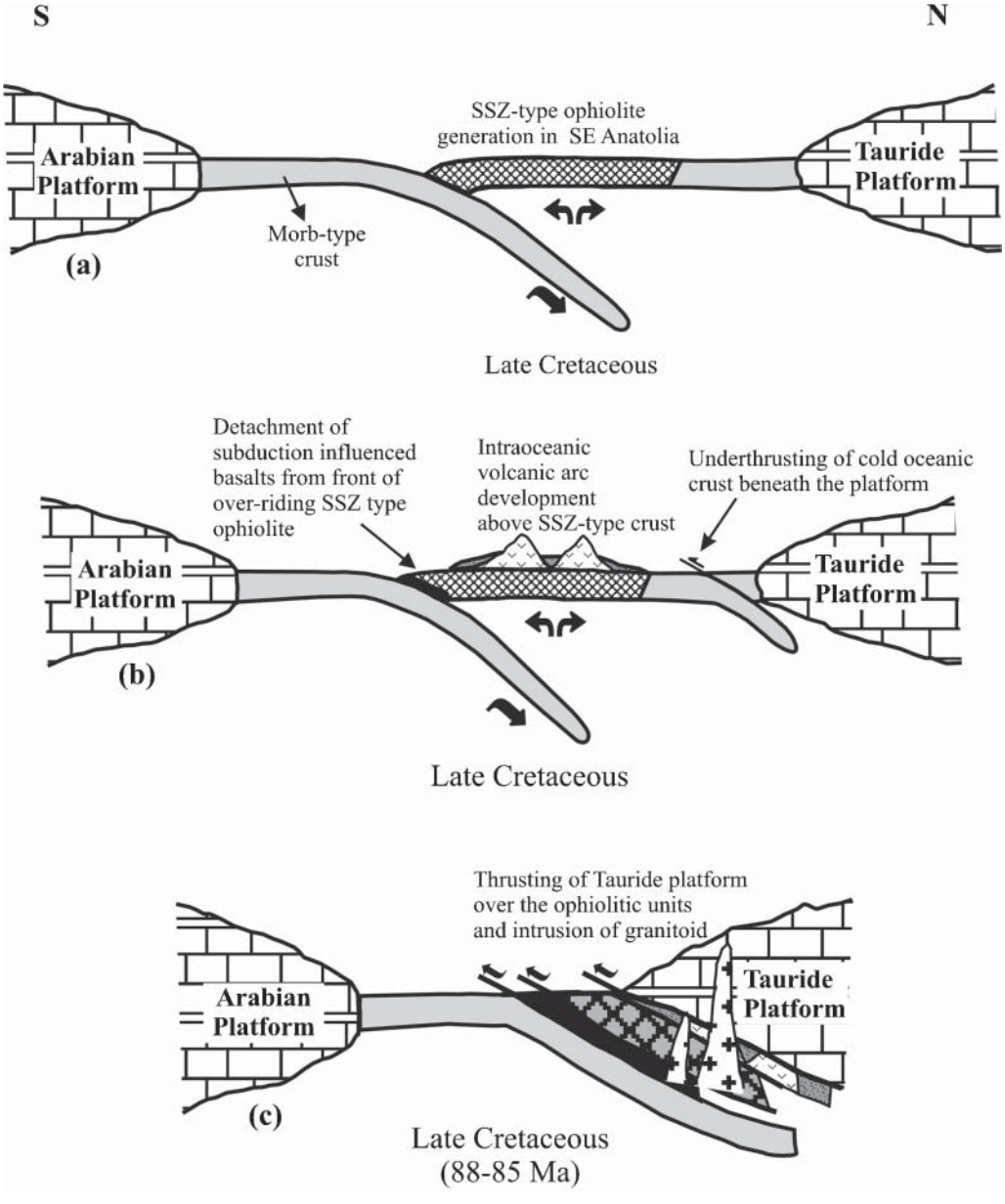

Fig. 15. Tectonic model for the genesis of the ophiolites, related metamorphic units and granitoids in SE Anatolia. (See text for discussion.).

of plagioclase observed in the amphibole gabbro. The amphibole gabbros are widespread in central Anatolia and are interpreted as being formed from a wet magma by high-degree partial melting of peridotite in a subduction-related setting (Koçak *et al.* 2005). High-level amphibole-bearing gabbros are reported from other eastern Mediterranean ophiolites (Hébert & Laurent 1990) and island-arc settings (Debari & Coleman 1989). Water-rich magmas are observed in arc regions where amphiboles commonly form (Arculus & Wills 1980). The geochemical evidence from the volcanic and plutonic rocks of the Kömürhan ophiolite shows that these are cogenetic tholeiitic suites formed in an SSZ tectonic setting during the Late Cretaceous in the southern branch of Neotethys. The metamorphic sole rocks of the Kömürhan ophiolite

exhibit a tholeiitic (Nb/Y = 0.07–0.33) nature. The REE patterns, multi-element and tectonomagmatic discrimination diagrams suggest that the protolith is akin to IAT.

The granitic rocks related to the evolution of the southern Neotethys in SE Anatolia are observed at three localities the Göksun–Afşin (Kahramanmaraş), Doğanşehir (Malatya) and Baskil (Elazığ) regions (Asutay 1988; Yazgan & Chessex 1991; Akgül 1993; Önal 1995; Parlak 2006; Robertson *et al*. 2006, 2007), as intruding the tectonostratigraphic–magmatic units of the nappe zone (Yılmaz 1993). The most important point is that the granitic rocks are seen to intrude all of the Malatya–Keban platform, the ophiolites and the related metamorphic units, suggesting that the Malatya–Keban platform and ophiolitic units were tectonically juxtaposed before the intrusion took place in the Late Cretaceous (Yazgan & Chessex 1991). The K–Ar isotopic age determinations on the granitic rocks of the region range from 76 ± 2.45 to 78 ± 2.5 Ma for the Baskil (Elazığ) area (Yazgan & Chessex 1991) and from 85.76 ± 3.17 to 70.05 ± 1.75 Ma for the Göksun (Kahramanmaraş) area (Parlak 2006). This suggests that the granite intrusion may be only slightly younger than the formation of the ophiolites (*c*. 90 Ma) (Mukasa & Ludden 1987; Robertson *et al*. 2006). Moreover, the field evidence throughout the region shows that the ophiolites and related metamorphic rocks were accreted to the base of the Malatya–Keban platform before intrusion took place.

A number of alternative tectonic models have been proposed to explain the genesis and emplacement of the ophiolites and the granitoid magmatism in the region. These are a the 'single subduction zone' model (Hall 1976; Aktaş & Robertson 1984, 1990; Robertson 1998, 2000; Yılmaz 1993; Yılmaz *et al*. 1993), a 'double subduction zone' model (Robertson 1998, 2000, 2002; Parlak *et al*. 2004) and a 'multi-phase convergence' model (Robertson *et al*. 2007). The field, geochemical and geochronological evidence from the Elazığ as well as the Kahramanmaraş (Parlak & Rızaoğlu 2004; Parlak 2006) and Malatya regions are consistent with the 'multiphase convergence' model of Robertson *et al*. (2006, 2007). The following evolutionary scenario based on this model is proposed for the tectonomagmatic units discussed above. The Kömürhan ophiolite was formed above a north-dipping subduction zone between the Arabian platform to the south and the Tauride platform to the north in the Late Cretaceous (*c*. 90 Ma) (Fig. 15a). Following this, an ensimatic island-arc assemblage was constructed on SSZ-type crust (Fig. 15b). The metamorphic sole was formed by the metamorphism of IAT-type basalts that were detached from the front of the overriding Kömürhan ophiolite and then underplated (Fig. 15b). Northward underthrusting of cold oceanic crust (possibly Early Mesozoic in age) was then initiated beneath the Tauride platform to the north (Fig. 15b). The Kömürhan ophiolite, the related metamorphic rocks and the volcano-sedimentary unit were then accreted to the base of the Tauride active margin in the north, where all the units were cut by the Baskil granitic rocks around 88–85 Ma (Fig. 15c).

Conclusions

(1) Major, trace and rare earth element geochemistry of the volcanic and subvolcanic rocks, as well as the mineral chemistry of the cumulate rocks from the Kömürhan ophiolite, suggest that they formed in an SSZ tectonic setting in the southern Neotethys during Late Cretaceous time. The presence of highly evolved rocks in the volcanic (andesite–dacite), sheeted dyke (microdiorite, quartz microdiorite), isotropic gabbro (diorite, quartz diorite) and cumulate gabbro (amphibole gabbro), as well as the high Ca-plagioclase in the mafic cumulate units are an indication of hydrous conditions, related to subduction.

(2) The metamorphic sole of the Kömürhan ophiolite was derived from metamorphism of an IAT-type basaltic protolith during intraoceanic thrusting–subduction. The volcanic rocks were presumably detached from the front of the overriding SSZ-type crust and then underplated and metamorphosed.

(3) The widespread volcanic–sedimentary unit (*c*. 750 m thick) in the Baskil (Elazığ) area exhibits alternations of basic to acidic extrusive rocks, debris flows, volcaniclastic sandstones and pelagic limestones. This unit is interpreted as a tholeiitic ensimatic island-arc assemblage, and has no genetic link with the Baskil granitic rocks. This unit was formed during a mature stage of SSZ spreading as the upper part of the Late Cretaceous Kömürhan ophiolite.

(4) The granitic rocks of the Baskil (Elazığ) region are observed as intruding the ophiolites, the volcanic–sedimentary unit and the Malatya–Keban platform. This suggests that the ophiolites and the volcanic–sedimentary unit were accreted to the base of the Malatya–Keban platform before the intrusions of the volcanic arc-type granitic bodies (i.e. Baskil, Doğanşehir and Göksun) around 88–85 Ma in SE Anatolia (Parlak 2006).

This work is a part of a PhD study by T. Rızaoğlu. Financial support from TÜBİTAK (Scientific and Technical Research Council of Turkey, Project No. 102Y041) and Niğde University Research Foundation (Project No. FBE2002–08) is gratefully acknowledged. We would like to thank F. Capponi for performing major and trace element analyses. We are grateful to M. Delaloye for thoughtful discussions on the evolution of the eastern Mediterranean ophiolites. D. Topa is thanked for his guidance during the microprobe analysis at Salzburg University (Austria). O. Parlak gratefully acknowledges the financial support of TÜBA (Turkish Academy of Sciences) in the frame of the Young Scientist Award Programme. A. H. F. Robertson, M. Delaloye and E. Yiğitbaş are thanked for their constructive reviews that improved the quality of the present paper.

References

Akgül, B. 1993. *Petrographical and petrological features of magmatic rocks in the vicinity of Piran village (Keban-Elazığ)*. PhD thesis, Fırat University, Elazığ, Turkey.

Aktaş, G. & Robertson, A. H. F. 1984. The Maden complex, SE Turkey: evolution of a Neotethyan continental margin. *In*: Dixon, J. E. & Robertson, A. H. F. (eds) *The Geological Evolution of the Eastern Mediterranean*. Geological Society, London, Special Publications, **17**, 375–402.

Aktaş, G. & Robertson, A. H. F. 1990. Tectonic evolution of the Tethys suture zone in SE Turkey: evolution evidence from the petrology and geochemistry of late Cretaceous and middle Eocene extrusives. *In*: Malpas, J., Moores, E., Panayiotou, A. & Xenophontos, C. (eds) *Ophiolites-Oceanic Crustal Analogues. Proceedings of the Troodos Ophiolite Symposium*. Geological Survey, Cyprus 1987, 311–329.

Alabaster, T., Pearce, J. A. & Malpas, J. 1982. The volcanic stratigraphy and petrogenesis of the Oman ophiolite complex. *Contributions to Mineralogy and Petrology*, **81**, 168–183.

Al-Riyami, K., Robertson, A. H. F., Dixon, J. & Xenophontos, C. 2002. Origin and emplacement of the Late Cretaceous Baer–Bassit ophiolite and its metamorphic sole in NW Syria. *Lithos*, **65**, 225–60.

Arculus, R. J. & Powell, R. 1986. Source component mixing in the regions of arc magma generation. *Journal of Geophysical Research*, **91**, 5913–5926.

Arculus, R. J. & Wills, K. J. A. 1980. The petrology of plutonic blocks and inclusions from the Lesser Antilles island arc. *Journal of Petrology*, **21**, 743–799.

Asutay, H. J. 1988. The geology of Baskil (Elazığ) vicinity and petrology of Baskil magmatics. *Bulletin of Mineral Research and Exploration (Ankara, Turkey)*, **107**, 46–72.

Bağci, U., Parlak, O. & Höck, V. 2006. Geochemical character and tectonic environment of ultramafic to mafic cumulates from the Tekirova (Antalya) ophiolite (southern Turkey). *Geological Journal*, (in press).

Beyarslan, M. 1996. *Kömürhan ofiyolit Biriminin Petrografik ve Petrolojik Özellikleri*. PhD thesis, Fırat Üniversitesi, Elazığ, Turkey.

Beyarslan, M. & Bingöl, A. F. 1996. The geochemistry and petrology of Elazığ magmatics. *In*: Korkmaz, S. & Akçay, M. (eds) *30th Annual Symposium Proceedings*. Karadeniz Teknik Üniversitesi, Trabzon, Turkey, 208–224.

Beyarslan, M. & Bingöl, A. F. 2000. Petrology of a supra-subduction zone ophiolite (Elazığ, Turkey). *Canadian Journal of Earth Sciences*, **37**, 1411–1424.

Bingöl, A. F. 1984. Geology of the Elazığ area in the eastern Taurus region. *In*: Tekeli, O. & Göncüoğlu, M. C. (eds) *The Geology of the Taurus Belt. International Symposium Proceedings, Ankara, Turkey*. MTA, Ankara 209–216.

Bölücek, C., Akgül, M. & Türkmen, İ. 2004. Volcanism, sedimentation and massive sulfide mineralization in a Late Cretaceous arc-related basin, Eastern Taurides, Turkey. *Journal of Asian Earth Sciences*, **24**, 349–360.

Bortolotti, V., Chiari, M., Marcucci, M., Marroni, M., Pandolfi, L., Principi, G. & Saccani, E. 2004. Comparison among the Albanian and Greek ophiolites: in research of constraints for the evolution of the Mesozoic Tethys ocean. *Ofioliti*, **29**, 19–35.

Debari, S. M. & Coleman, R. G. 1989. Examination of the deep levels of an island arc: evidence from the Tonsina ultramafic–mafic assemblage, Tonsina, Alaska. *Journal of Geophysical Research*, **94**, 4373–4391.

Desmons, J., Delaloye, M., Desmet, A., Gagny, C., Rocci, G. & Voldet, P. 1980. Trace and REE abundance in Troodos lavas and sheeted dykes, Cyprus. *Ofioliti*, **5**, 35–56.

Droop, G. T. R. 1987. A general equation of estimating Fe^{3+} concentrations in ferromagnesian silicates and oxides from microprobe analyses using stoichiometric criteria. *Mineralogical Magazine*, **51**, 431–435.

Erdem, E. & Bingöl, A. F. 1995. Pütürge (Malatya) metamorfitlerinin petrografik özellikleri. *Fırat Üniversitesi Mühendislik Fakültesi Dergisi*, **7**, 73–85.

Erdoğan, B. 1977. *Geology, geochemistry and genesis of the sulfide deposits of the Ergani–Maden region, SE Turkey*. PhD thesis, New Brunswick University Brunswick.

Floyd, P. A. & Winchester, J. A. 1975. Magma type and tectonic setting discrimination using immobile elements. *Earth and Planetary Science Letters*, **27**, 211–218.

Floyd, P. A. & Winchester, J. A. 1978. Identification and discrimination of altered and metamorphosed volcanic rocks using immobile elements. *Chemical Geology*, **21**, 291–306.

Floyd, P. A., Kelling, G. & Gökçen, S. 1991. Geochemistry and tectonic environment of basaltic rocks from the Misis ophiolitic melange, south Turkey. *Chemical Geology*, **89**, 263–280.

Foden, J. D. 1983. The petrology of calcalkaline lavas of Rindjani volcano, East Sunda Arc: model for island arcs. *Journal of Petrology*, **24**, 98–130.

FUJIMAKI, H. 1986. Fractional crystallization of the basaltic suite of Usa volcano, southwest Hokkaido, Japan, and its relationships with the associated felsic suite. *Lithos*, **19**, 129–140.

GUST, D. A. & JOHNSON, R. W. 1981. Amphibole bearing cumulates from Boisa island, Papua New Guinea: evaluation of the role of fractional crystallization in an andesitic volcano. *Journal of Geology*, **89**, 219–232.

HALL, R. 1976. Ophiolite emplacement and the evolution of the Taurus suture zone, southeast Turkey. *Geological Society of America Bulletin*, **87**, 1078–1088.

HART, S. R., ERLANK, A. J. & KABLE, E. J. D. 1974. Sea floor basalt alteration: some chemical and Sr isotopic effects. *Contributions to Mineralogy and Petrology*, **44**, 219–230.

HÉBERT, R. & LAURENT, R. 1990. Mineral chemistry of the plutonic section of the Troodos ophiolite: new constraints for genesis of arc-related ophiolites. *In*: MALPAS, J., MOORES, E. M., PANAYIOTOU, A. & XENOPHONTOS, C. (eds) *Ophiolites—Oceanic Crustal Analogues. Proceedings of Troodos Ophiolite Symposium, Cyprus Geological Survey 1987*, 149–163.

HEMPTON, M. R. 1984. Results of detailed mapping near Lake Hazar (Eastern Taurus Mountains). *In*: TEKELİ, O. & GÖNCÜOĞLU, M. C. (eds) *Geology of the Taurus Belt. Proceedings of International Symposium, 26–29 September 1983, Ankara, Turkey*. MTA, Ankara, 223–228.

HEMPTON, M. R. 1985. Structure and deformation history of the Bitlis suture near Lake Hazar, SE Turkey. *Geological Society of America Bulletin*, **96**, 223–243.

HUMPRIES, S. E. & THOMPSON, G. 1978. Trace element mobility during hydrothermal alteration of oceanic basalts. *Geochimica et Cosmochimica Acta*, **42**, 127–136.

JENNER, G. A., DUNNLNG, G. R., MALPAS, J., BROWN, M. & BRACE, T. 1991. Bay of Islands and Little Port complexes revisited: age, geochemical and isotopic evidence confirm suprasubduction-zone origin. *Canadian Journal of Earth Sciences*, **28**, 1635–1652.

KOÇAK, K., IŞIK, F., ARSLAN, M. & ZEDEF, V. 2005. Petrological and source characteristics of ophiolitic hornblende gabbros from the Aksaray and Kayseri regions, central Anatolian crystalline complex, Turkey. *Journal of Asian Earth Sciences*, **25**, 883–891.

MESCHEDE, M. 1986. A method of discriminating between different types of mid-oceanic ridge basalts and continental tholeiites with Nb–Zr–Y diagram. *Chemical Geology*, **56**, 207–218.

MICHARD, A., JUTEAU, T. & WHITECHURCH, H. 1985. L'obduction: revue des modeles et confrontation au cas de l'Oman. *Bulletin de la Société Geologique de France*, **2**, 189–198.

MTA. 2002. *1/500 000 scale geological maps of Turkey*. General Directorate of Mineral Research and Exploration, Ankara.

MUKASA, S. B. & LUDDEN, J. N. 1987. Uranium–lead ages of plagiogranites from the Troodos ophiolite, Cyprus, and their tectonic significance. *Geology*, **1**, 825–828.

ÖNAL, A. 1995. *Polat-Beğre (Doğanşehir–Malatya) Çevresindeki magmatik kayaçların petrografik ve petrolojik özellikleri*. PhD thesis, Fırat Üniversitesi, Elazığ, Turkey.

PARLAK, O. 1996. *Geochemistry and geochronology of the Mersin ophiolite within the eastern Mediterranean tectonic frame*. PhD thesis, University of Geneva.

PARLAK, O. 2006. Geodynamic significance of granitoid magmatism in southeast Anatolia: Geochemical and geochronological evidence from Göksun–Afşin (Kahramanmaraş, Turkey) region. *International Journal of Earth Sciences* (in press).

PARLAK, O. & ROBERTSON, A. H. F. 2004. Tectonic setting and evolution of the ophiolite-related Mersin Mélange, southern Turkey: its role in the tectonic–sedimentary setting of the Tethys in the eastern Mediterranean region. *Geological Magazine*, **141**, 257–286.

PARLAK, O. & RIZAOĞLU, T. 2004. Geodynamic significance of granitoid intrusions in the southeast Anatolian Orogeny (Turkey) *In*: CHATZIPETROS, A. A. & PAVLIDES, S. B. (eds) *Proceedings of the 5th International Eastern Mediterranean Geology Symposium*, Thessaloniki, Greece, 14–20 April 2004, 157.

PARLAK, O., DELALOYE, M. & BINGÖL, E. 1996. Mineral chemistry of ultramafic and mafic cumulates as an indicator of the arc-related origin of the Mersin ophiolite (southern Turkey). *Geologische Rundschau*, **85**, 647–661.

PARLAK, O., HÖCK, V. & DELALOYE, M. 2000. Suprasubduction zone origin of the Pozanti–Karsanti ophiolite (southern Turkey) deduced from whole-rock and mineral chemistry of the gabbroic cumulates. *In*: BOZKURT, E., WINCHESTER, J. A. & PIPER, J. D. A. (eds) *Tectonics and Magmatism in Turkey and the Surrounding Area.* Geological Society, London, Special Publications, **173**, 219–234.

PARLAK, O., HÖCK, V., KOZLU, H. & DELALOYE, M. 2004. Oceanic crust generation in an island arc tectonic setting, SE Anatolian Orogenic Belt (Turkey). *Geological Magazine*, **141**, 583–603.

PEARCE, J. A. 1982. Trace element characteristics of lavas from destructive plate boundaries. *In*: THORPE, R. S. (ed) *Andesites: Orogenic Andesites and Related Rocks*. Wiley, Chichester, 525–548.

PEARCE, J. A. 1983. Role of the subcontinental lithosphere in magma genesis at active continental margins. *In*: HAWKESWORTH, C. J. & NORRY, M. J. (eds) *Continental Basalts and Mantle Xenoliths.* Shiva, Nautwich, 230–249.

PEARCE, J. A. 1996. A users guide to basalt discrimination diagrams. *In*: WYMAN, D. A. (ed) *Trace Element Geochemistry of Volcanic Rocks: Applications for Massive Sulphide Exploration*. Geological Association of Canada, Short Course Notes, **12**, 79–113.

PEARCE, J. A. & CANN, J. R. 1973. Tectonic setting of basaltic volcanic rocks determined using trace element analysis. *Earth and Planetary Science Letters*, **19**, 290–300.

PEARCE, J. A. & NORRY, M. J. 1979. Petrogenetic implications of Ti, Zr, Y and Nb variations in volcanic rocks. *Contributions to Mineralogy and Petrology*, **69**, 33–47.

PEARCE, J. A., LIPPARD, S. J. & ROBERTS, S. 1984. Characteristics and tectonic significance of suprasubduction zone ophiolites. *In*: KOKELAAR, B. P. & HOWELLS, M. F. (eds) *Marginal Basin Geology*. Geological Society, London, Special Publications, **16**, 77–94.

PEATE, D. W., PEARCE, J. A., HAWKESWORTH, C. J., COLLEY, H., EDWARDS, C. M. H. & HIROSE, K. 1997. Geochemical variations in Vanuatu island arc lavas: the role of the subducted material and a variable mantle wedge composition. *Journal of Petrology*, **38**, 1331–1358.

PERİNÇEK, D. 1979. *The geology of Hazro–Koruda–Çüngüş–Maden–Ergani–Hazar–Elazığ–Malatya area. Ankara, Turkey*. Türkiye Jeoloji Kurumu Yayını, Ankara.

RIZAOĞLU, T., PARLAK, O. & İŞLER, F. 2004. Geochemistry and tectonic setting of the Kömürhan ophiolite in southeast Anatolia. *In*: CHATZIPETROS, A, A. & PAVLIDES, S. B. (eds) *Proceedings of the 5th International Eastern Mediterranean Geology Symposium*, 14–20 April 2004, Thessaloniki, Greece, 285.

ROBERTSON, A. H. F. 1998. Mesozoic–Tertiary tectonic evolution of the easternmost Mediterranean area; integration of marine and land evidence. *In*: ROBERTSON, A. H. F., EMEIS, K. C., RICHTER, K. C. & CAMERLENGHI, A (eds) *Proceeding of Ocean Drilling Program, Scientific Results, **160***. Ocean Drilling Program, College Stating TX, 723–782.

ROBERTSON, A. H. F. 2000. Mesozoic–Tertiary tectonic–sedimentary evolution of a south Tethyan oceanic basin and its margins in southern Turkey. *In*: BOZKURT, E., WINCHESTER, J. A. & PIPER, J. D. A. (eds) *Tectonics and Magmatism in Turkey and the Surrounding Area*. Geological Society, London, Special Publications, **173**, 97–138.

ROBERTSON, A. H. F. 2002. Overview of the genesis and emplacement of Mesozoic ophiolites in the Eastern Mediterranean Tethyan region. *Lithos*, **65**, 1–67.

ROBERTSON, A. H. F. 2004. Development of concepts concerning the genesis and emplacements of Tethyan ophiolites in the eastern Mediterranean and Oman regions. *Earth-Science Reviews*, **66**, 331–387.

ROBERTSON, A. H. F., USTAÖMER, T., PARLAK, O., ÜNLÜGENÇ, U. C., TASLI, K. & İNAN, N. 2006. The Berit transect of the Tauride thrust belt, S. Turkey: Late Cretaceous–Early Cenozoic accretionary/collisional processes related to closure of the Southern Neotethys. *Journal of Asian Earth Sciences* (in press).

ROBERTSON, A. H. F., PARLAK, O., RIZAOĞLU, T., ÜNLÜGENÇ, U. C., İNAN, N., TASLI, K. & USTAÖMER, T. 2007. Late Cretaceous–Mid Tertiary tectonic evolution of the eastern Taurus mountains and the southern Tethyan ocean; evidence from the Elazığ region, SE Turkey. *In*: RIES, A. C., BUTLER, R. W. H. & GRAHAM, R. H. (eds) *Deformation of the Continental Crust*, Geological Society, London, Special Publications (in press).

ROLLINSON, H. 1993. *Using Geochemical Data: Evaluation, Presentation, Interpretation*. Longman, Harlow.

SEARLE, M. P., LIPPARD, S. J., SMEWING, J. D. & REX, D. C. 1980. Volcanic rocks beneath the Semail ophiolite nappe in the northern Oman mountains and their significance in the Mesozoic evolution of Tethys. *Journal of the Geological Society, London*, **137**, 589–604.

ŞENGÖR, A. M. C. & YILMAZ, Y. 1981. Tethyan evolution of Turkey: plate tectonic approach. *Tectonophysics*, **75**, 181–241.

STERN, R. J. 1979. On the origin of andesite in the northern Mariana island arc: implications from Agrigan. *Contributions to Mineralogy and Petrology*, **68**, 207–219.

SUN, S. S. & MCDONOUGH, W. F. 1989. Chemical and isotopic systematics of oceanic basalts: implications for mantle composition and processes. *In*: SAUNDERS, A. D. & NORRY, M. J. (eds) *Magmatism in the Ocean Basins.* Geological Society, London, Special Publications, **42**, 313–347.

TURAN, M. & BİNGÖL, A. F. 1991. Tectono-stratigraphic characteristics of the region between Kovancılar–Baskil, Elazığ, Turkey. *In*: YETİŞ, C. (ed.) *Proceedings of Ahmet Acar Geology Symposium*. Çukurova University, Adana, Turkey, 213–227.

WALLIN, E. T. & METCALF, R. V. 1998. Suprasubduction zone ophiolites formed in an extensional forearc: Trinity terrane, Klamath mountains, California. *Journal of Geology*, **106**, 591–608.

WOOD, D. A., JORON, J. L. & TREUIL, M. 1979. A reappraisal of the use of trace elements to classify and discriminate between magma series erupted in different tectonic settings. *Earth and Planetary Science Letters*, **45**, 326–336.

YALINIZ, K. M., FLOYD, P. & GÖNCÜOĞLU, M. C. 1996. Supra-subduction zone ophiolites of Central Anatolia: geochemical evidence from the Sarikaraman ophiolite, Aksaray, Turkey. *Mineralogical Magazine*, **60**, 697–710.

YALINIZ, K. M., FLOYD, P. & GÖNCÜOĞLU, M. C. 2000. Geochemistry of volcanic rocks from the Çiçekdağ ophiolite, Central Anatolia, Turkey, and their inferred tectonic setting within the northern branch of the Neotethyan ocean. *In*: BOZKURT, E., WINCHESTER, J. A. & PIPER, J. D. A. (eds) *Tectonics and Magmatism in Turkey and the Surrounding Area.* Geological Society, London, Special Publications, **173**, 203–218.

YAZGAN, E. 1983. A geotraverse between the Arabian platform and the Munzur mountains. *Field Guide Book, Excursion. 5th International Symposium on Geology of the Taurus Belt, Ankara*. MTA Ankara.

YAZGAN, E. 1984. Geodynamic evolution of the eastern Taurus. *In*: TEKELİ, O. & GÖNCÜOĞLU, M. C. (eds) *The Geology of the Taurus Belt. Proceedings of the International Symposium, Ankara*, 199–208. MTA Ankara.

YAZGAN, E. & CHESSEX, R. 1991. Geology and tectonic evolution of the southeastern Taurides in the region of Malatya. *Bulletin of Turkish Association of Petroleum Geologists*, **3**, 1–42.

YİĞİTBAŞ, E. & YILMAZ, Y. 1996*a*. New evidence and solution to the Maden complex controversy of the southeast Anatolian orogenic belt (Turkey). *Geologische Rundschau*, **85**, 250–263.

YİĞİTBAŞ, E. & YILMAZ, Y. 1996*b*. Post-late Cretaceous strike-slip tectonics and its implications on the Southeast Anatolian orogen, Turkey. *International Geology Review*, **38**(9), 818–831.

YILDIRIM, M. & YILMAZ, Y. 1991. Güneydoğu Anadolu orojenik kuşağının ekaylı zonu. *Bulletin of Turkish Association of Petroleum Geologists*, **3**, 57–73.

YILMAZ, O. 1971. *Etude pétrographique et géochronologique de la région de Cacas*. PhD thesis, Université Science et Médicale de Grenoble.

YILMAZ, Y. 1978. Bitlis massif and ophiolite relationship around Gevaş, Van. *Proceedings of 4th Petroleum Congress of Turkey, Ankara*, 88–93. TPJD, Ankara.

YILMAZ, Y. 1993. New evidence and model on the evolution of the southeast Anatolian orogen. *Geological Society of America Bulletin*, **105**, 251–271.

YILMAZ, Y., GÜRPINAR, O., KOZLU, H., *et al*. 1987. *Kahramanmaraş Kuzeyinin Jeolojisi (Andırın–Berit–Engizek–Nurhak–Binboğa Dağları)*. Türkiye Petrolleri A.O. Rapor, **2028**.

YILMAZ, Y., YİĞİTBAŞ, E. & GENÇ, Ş. C. 1993. Ophiolitic and metamorphic assemblages of southeast Anatolia and their significance in the geological evolution of the orogenic belt, *Tectonics*, **12**, 1280–1297.

YOGODZINSKI, G. M., VOLYNETS, O. N., KOLOSKOV, A. V., SELIVERSTOV, N. I. & MATVENKOV, V. V. 1993. Magnesian andesites and the subduction component in strongly calc-alkaline series at Piip volcano, far western Aleutians. *Journal of Petrology*, **35**, 163–204.